https://doi.org/10.5194/acp-2020-1295
Preprint. Discussion started: 15 March 2021

Atmospheric Chemistry and Physics Discussions

Study of Different Carbon Bond 6 (CB6) Mechanisms by Using a Concentration Sensitivity Analysis

Le Cao, Simeng Li, and Luhang Sun

Key Laboratory for Aerosol-Cloud-Precipitation of China Meteorological Administration, Nanjing University of Information Science and Technology, Nanjing, China

Correspondence: L. Cao
(le.cao@nuist.edu.cn)

Abstract. Since the year 2010, different versions of the Carbon Bond 6 (CB6) mechanism have been developed, to accurately estimate the contribution to the air pollution by the chemistry. However, the discrepancies in simulation results brought about by the modifications between different versions of the CB6 mechanism are still not fully understood. Therefore, in the present study, we investigated the behavior of three different CB6 mechanisms (CB6r1, CB6r2 and CB6r3) in simulating ozone (O_3), nitrogen oxides (NO_x) and formaldehyde (HCHO) under an urban condition, by applying a concentration sensitivity analysis in a box model. The results show that when the surface emission is excluded, the O_3 level predicted by CB6r1 is approximately 6% and 8% higher than that predicted by CB6r2 and CB6r3, specifically due to the change in the sink of CXO3 in the mechanism. In contrast, the levels of NO_x and HCHO estimated by these three CB6 mechanisms are mostly similar, when the surface emission is turned off. After adding the surface emission, the simulated profiles of O_3, NO_x and HCHO obtained by CB6r2 and CB6r3 are similar. However, the deviation between the O_3 levels provided by CB6r1 and the other two CB6 mechanisms (i.e. CB6r2 and CB6r3) is enlarged, because of the weakening of the ozone dependence on the emission of isoprene in CB6r1. Moreover, HCHO predicted by CB6r1 is found larger than that predicted by CB6r2 and CB6r3, which is caused by an enhanced dependence of HCHO on the emission of isoprene in CB6r1. Regarding to NO_x, it was found that CB6r1 gives a higher value during the daytime and a lower value during the nighttime than the other two mechanisms, which is caused by the relatively stronger connection between the NO_x prediction and the local chemistry in CB6r1, so that more NO_x is consumed and converted to PANX (peroxyacyl nitrate with three and higher carbons) in the nighttime and more NO_x is reformed by the photolysis of PANX in the daytime.

1 Introduction

Air pollution occurs when the concentration of particles or gases in the atmosphere exceeds a standard, causing a harmful effect to the human beings and the environment of the earth. It was estimated that in 2007, approximately 3.45 million people were killed worldwide due to the air pollution (Zhang et al., 2017a). Thus, it is needed to investigate the physicochemical properties of the air pollution so that the formulation of the control strategy by the government can be guided.

Atmospheric transport model (ATM) is an efficient tool for revealing the factors dominating the air pollution. Usually the ATM includes a variety of processes that are responsible for the concentration change of pollutants in the air, such as the

https://doi.org/10.5194/acp-2020-1295
Preprint. Discussion started: 15 March 2021

Atmospheric Chemistry and Physics Discussions

production/consumption by the local chemistry, horizontal advection and vertical convection. By using ATMs, the contribution to the concentration change of the pollutants by each process can be numerically estimated.

Gas-phase chemical reaction mechanism is an essential part of the ATM. It can transform the emissions and the chemical reactions occurring in the atmosphere into the corresponding change of the species, which enables following computations of the ATM. To the present, several atmospheric gas-phase chemical reaction mechanisms have been proposed, such as the detailed Master Chemical Mechanism (MCM) (Jenkin et al., 1997, 2003, 2012, 2015; Saunders et al., 2003; Bloss et al., 2005) and the global chemical transport model MOZART (Model for Ozone and Related chemical Tracers) mechanism (Emmons et al., 2010). Among these chemical mechanisms, condensed mechanisms such as Carbon Bond Mechanisms (Gery et al., 1989; Zaveri and Peters, 1999; Yarwood et al., 2005, 2010) and SAPRC mechanisms (Carter, 2000a,b, 2010) are widely applied in ATMs due to their relatively small size and adequate accuracy. In these condensed mechanisms, different techniques are used to lump volatile organic compounds (VOCs) into functional groups while the treatment of the inorganic chemistry is mostly similar.

Carbon Bond Mechanism (CBM) is a kind of condensed mechanism, which lumps VOCs by chemical moiety (Stockwell et al., 2019). In CBM mechanisms, the carbon bond is treated as a reaction unit, and the carbon bonds with the same bonding state are treated as a group, while the exact location of the carbon bonds in the molecule is neglected. CBM is conveniently implemented in the ATMs because of its small size and high accuracy in predicting the concentration change of the pollutants. However, due to the lumping technique, biases are inevitably brought into computations. Thus, many updates were made to the CBM mechanism to reduce biases, such as adding an explicit representation of species with the same molecular type (e.g. species ALDX for higher-order aldehydes).

As mentioned above, CBM mechanism has been updated for several generations. In 1989, CB-IV was proposed by Gery et al. (1989), and it was then widely used in many air quality models such as WRF-Chem (Grell et al., 2005) and CMAQ (Byun and Schere, 2006). In 2005, based on the CB-IV mechanism, Yarwood et al. (2005) released CB05 by explicitly adding higher order aldehydes and internal olefins into the mechanism. A large amount of smog chamber experiments were also used to validate CB05, and it was reported that CB05 behaves better than CB-IV against the chamber data (Yarwood et al., 2005). Later on, an update to CB05 was made by Whitten et al. (2010) by combining a new toluene mechanism with CB05, namely CB05TU mechanism. It was proved that the CB05TU mechanism improves upon the CB05 mechanism in simulating toluene related reactions (Whitten et al., 2010).

The latest version of the CBM mechanism is CB6 (Yarwood et al., 2010), because it is the 6-th generation of this mechanism family, and it was released to deal with the tightening of the ozone standard in the US. Long-lived and relatively abundant organic compounds formed by peroxy radical reactions (RO_2-RO_2) are taken into account in CB6. Moreover, the isoprene chemistry and the aromatic chemistry are extensively revised, to improve the modeling of the formation of secondary organic aerosols (SOAs). It was shown that CB6 performs better in simulating the maximum value of ozone as well as the ozone formation rate compared with the CB05 mechanism (Yarwood et al., 2010). From then on, several updates were made to CB6 so that currently there are four versions of CB6 available, i.e. CB6r1, CB6r2, CB6r3 and CB6r4. In CB6r1, the mechanism previously proposed by Yarwood et al. (2010) was revised again (Yarwood et al., 2012), and several reactions and products were corrected.

https://doi.org/10.5194/acp-2020-1295
Preprint. Discussion started: 15 March 2021

Atmospheric Chemistry and Physics Discussions

New experimental data (EUPHORE experiments) were also adopted to validate the CB6r1 mechanism (Yarwood et al., 2012). After that, in 2013, Ruiz Hildebrandt and Yarwood (2013) included the interactions between organic aerosols and total reactive nitrogen (NO_y) in the mechanism, and then gave the CB6r2 mechanism. In CB6r2, organic nitrates were divided into two groups, simple alkyl nitrates (NTR1) that remain in the gas phase and multi-functional nitrates (NTR2) that can partition into organic aerosols. Because of the inclusion of the multi-functional aerosol nitrates, lower recycling efficiency of nitrogen oxides (NO_x) from nitrates is acquired using CB6r2, leading to a lower ozone production relative to CB6r1 (Ruiz Hildebrandt and Yarwood, 2013). The third version of CB6 is CB6r3 (Emery et al., 2015), which was developed to account for the influence of the low temperature on the formation of organic nitrates. It aims at modeling the winter ozone formation event in Uinta Basin in the US under cold conditions, and it was found that the inclusion of the temperature dependence in CB6r3 would cause an ozone reduction in winter environments, due to an enhanced formation of organic nitrates. The latest version of the CB6 mechanism is CB6r4 (Emery et al., 2016), which was designed by combing CB6r3 with a 16-reaction skeletal iodine mechanism, to consider the ozone depletion by the iodine chemistry. It was found that CB6r2 and CB6r4 perform similarly in simulating ozone across the continental US, but CB6r4 tends to predict a lower ozone than CB6r2, possibly due to the depletion of ozone by the iodine chemistry in the marine boundary layer (Emery et al., 2016).

Many investigations have been made using the CB6 mechanisms. To name a few, Luecken et al. (2019) used CB6r3 to simulate ozone, oxidized nitrogen (NO_y) and hazardous air pollutants (HAPs) across the continental US. In their study, a comparison between CB6r3, CB05TU, and CB05 as well as the observational data was performed. It was shown that these chemical mechanisms behave similarly for the ozone prediction, and CB6r3 performs the best in simulating the vertical distribution of peroxyacyl nitrates. Marvin et al. (2017) used five chemical mechanisms including CB6r2 to evaluate the impact of the isoprene chemistry on the simulation of formaldehyde (HCHO) in the summertime southeast US. They also suggested a set of modifications to CB6r2 that can improve the comparison of the modeled HCHO to observations. Zhang et al. (2017b) used the Comprehensive Air Quality Model with Extensions (CAMx) (ENVIRON, 2015) with the implementation of the CB6r2 mechanism to estimate the biogenic isoprene emissions in US by using two different emission models, BEIS (Pierce et al., 1998; Bash et al., 2016) and MEGAN (Guenther et al., 2006, 2012), and they found that the MEGAN model predicts more isoprene emissions than the BEIS model.

Despite the studies mentioned above, the corresponding change brought about by the modifications between different versions of the CB6 mechanism is still unknown. The internal properties of these CB6 mechanisms such as the relationship between the ozone formation and the surface emission are also not thoroughly investigated and compared. Therefore, in this study, we performed a concentration sensitivity analysis on different versions of the CB6 mechanism (CB6r1, CB6r2, and CB6r3) to see the dependence of the formation of ozone (O_3), nitrogen oxides (NO_x, $NO+NO_2$) and formaldehyde (HCHO) on each reaction of the mechanism as well as the surface emission. By doing that, we were able to figure out the reasons causing the deviations between the results obtained by using different CB6 mechanisms. The factors dominating the formation and consumption of the focused species (O_3, NO_x and HCHO) in these mechanisms can also be revealed.

The structure of this paper is as follows. In Sect. 2, CB6 mechanisms used in this study are introduced, and the method used to analyze the mechanism as well as the governing equations are also described. Sect. 3 gives the results of the concentration

https://doi.org/10.5194/acp-2020-1295
Preprint. Discussion started: 15 March 2021

Atmospheric Chemistry and Physics Discussions

sensitivity analysis and the related discussions. In Sect. 4, major conclusions achieved in this study are summarized. Future work is also prospected in this section.

2 Description of the Mechanisms and the Numerical Method

In the present study, we first implemented different versions of the CB6 mechanism (i.e. CB6r1, CB6r2, and CB6r3) into a box model, KINAL (Turányi, 1990a), to simulate the temporal evolution of O_3, NO_x and HCHO under a typical urban condition. The surface emission was not included at first, so that chemical reactions playing an important role in the change of the focused species can be indicated. Then, sensitivities of the focused species (O_3, NO_x and HCHO) to each reaction of the mechanisms were computed, to reveal the influence brought about by the modifications between these CB6 mechanisms. Later, the surface emission was added into the model, and a same procedure was performed on these mechanisms again, so that the behavior of these CB6 mechanisms under a typical heavily polluted condition can be investigated.

The CB6 mechanisms studied in this paper contain approximately 80 chemical species and 220 reactions. The CB6r1 version contains 80 species and 222 reactions, and the CB6r2 version contains 81 species and 215 reactions. The CB6r3 version has 82 species and 221 reactions, including reactions accounting for the temperature dependence of the alkyl nitrate formation. Complete listings of all the reactions of these mechanisms are given in Tab. A1 of the appendix. The updates in CB6r2 and CB6r3 compared with their previous version are also marked in Tab. A1. Compared with CB6r1, CB6r2 divides the organic nitrates generated from alkanes, olefins, aromatics and oxygenated VOCs (i.e. the species named NTR in CB6r1) into two groups, NTR1 that exists exclusively in the gas phase and NTR2 that can partition into organic aerosols. As a result of this speciation, in CB6r2, the organic nitrates, NTR1 and NTR2, undergo the following reactions:

$$\mathrm{NTR1} + h\nu \rightarrow \mathrm{NO_2}, \tag{R1}$$

$$\mathrm{NTR1} + \mathrm{OH} \rightarrow \mathrm{NTR2}, \tag{R2}$$

$$\mathrm{NTR2} + \mathrm{H_2O_{(aerosol)}} \rightarrow \mathrm{HNO_3}. \tag{R3}$$

Reaction (R1) denotes the photolysis of NTR1, which enables a recycling of NO_x and a following ozone formation enhancement. Reaction (R2) represents an addition reaction leading to the conversion from NTR1 to NTR2. Reaction (R3) means that the organic nitrate partitioning within the aerosols undergoes hydrolysis and forms HNO_3. Ruiz Hildebrandt and Yarwood (2013) reported that because of this speciation, CB6r2 has a lower recycling efficiency of NO_x from organic nitrates. The levels of O_3 and NO_x predicted by CB6r2 are thus lower than those predicted by CB6r1.

Regarding to CB6r3, it decomposes the formation process of alkyl nitrates from alkanes in CB6r2:

$$\begin{aligned}\mathrm{PRPA} + \mathrm{OH} \rightarrow\ & 0.71\mathrm{ACET} + 0.26\mathrm{ALDX} + 0.26\mathrm{PAR} \\ & + 0.97\mathrm{XO2N} + 0.03\mathrm{XO2N} + \mathrm{RO2},\end{aligned} \tag{R4}$$

https://doi.org/10.5194/acp-2020-1295
Preprint. Discussion started: 15 March 2021


Atmospheric Chemistry and Physics Discussions

$$\mathrm{PAR} + \mathrm{OH} \rightarrow 0.11\mathrm{ALDX} + 0.76\mathrm{ROR} + 0.13\mathrm{XO2N} + 0.11\mathrm{XO2H} + 0.76\mathrm{XO2} + \mathrm{RO2} - 0.11\mathrm{PAR}, \quad \text{(R5)}$$

$$\mathrm{XO2N} + \mathrm{NO} \rightarrow 0.5\mathrm{NTR1} + 0.5\mathrm{NTR2}, \quad \text{(R6)}$$

into seven reactions:

$$\mathrm{PRPA} + \mathrm{OH} \rightarrow \mathrm{XPRP}, \quad \text{(R7)}$$

$$\mathrm{XPRP} \rightarrow \mathrm{XO2N} + \mathrm{RO2}, \quad \text{(R8)}$$

$$\mathrm{XPRP} \rightarrow 0.73\mathrm{ACET} + 0.268\mathrm{ALDX} + 0.268\mathrm{PAR} + \mathrm{XO2H} + \mathrm{RO2}, \quad \text{(R9)}$$

$$\mathrm{PAR} + \mathrm{OH} \rightarrow \mathrm{XPAR}, \quad \text{(R10)}$$

$$\mathrm{XPAR} \rightarrow \mathrm{XO2N}, \quad \text{(R11)}$$

$$\mathrm{XPAR} \rightarrow 0.126\mathrm{ALDX} + 0.874\mathrm{ROR} + 0.126\mathrm{XO2H} + 0.874\mathrm{XO2} + \mathrm{RO2} - 0.126\mathrm{PAR}, \quad \text{(R12)}$$

$$\mathrm{XO2N} + \mathrm{NO} \rightarrow 0.5\mathrm{NTR1} + 0.5\mathrm{NTR2}. \quad \text{(R13)}$$

By making this modification, the dependence of the alkyl nitrate yield on the pressure and the temperature can be considered in CB6r3, especially under cold conditions. For this purpose, two new operators, XPRP and XPAR, were added. Under a standard condition (pressure: 1 atm, temperature: 298 K), the formation of the alkyl nitrates (NTR1 and NTR2) in CB6r3 through Reactions (R7)-(R13) is equal to that in CB6r2 through Reactions (R4)-(R6).

https://doi.org/10.5194/acp-2020-1295
Preprint. Discussion started: 15 March 2021

Atmospheric Chemistry and Physics Discussions

CB6r4 improves upon CB6r3 by adding a condensed iodine mechanism to consider the iodine-induced ozone destruction (Emery et al., 2016). However, CB6r4 was not investigated in this study, because the halogen chemistry is not the focus of the present study. A comparison between CB6r4 and other CB6 mechanisms in a halogen-rich environment is attributed to a future work.

We implemented the CB6 mechanisms mentioned above into a box model, KINAL (Turányi, 1990a), to capture the time variations of O_3, NO_x and HCHO by solving Eq. (1):

$$\frac{\mathrm{d}\boldsymbol{c}}{\mathrm{d}t} = \boldsymbol{f}(\boldsymbol{c},\boldsymbol{k}) + \boldsymbol{E}. \tag{1}$$

In Eq. (1), $\boldsymbol{c}$ is a column vector of species concentrations. $\boldsymbol{k}$ is a vector of reaction rate constants and t denotes time. $\boldsymbol{E}$ represents a source term of the local surface emission, and in the present model the surface emission is parameterized as a group of reactions having products and a constant reaction rate but without reactants. KINAL is a box model provided for the analysis of complex reaction systems. Stiff kinetic differential equations can be solved in KINAL, and it was proved that KINAL performs robustly and efficiently (Turányi, 1990a,b; Cao et al., 2014, 2016, 2019). A scenario with a typical urban background air composition (see Tab. 1) adopted from Saylor and Ford (1995) and Sandu et al. (1997) was simulated. The simulation scenario represents a heavily polluted atmosphere, in which the background level of NO_x is in the order of 1-1000 ppb, much higher than that under a rural condition. A 7-day simulation was performed and the simulation starts at noon (12:00) of the first day. The time variations of O_3, NO_x and HCHO were recorded every hour during the simulation period.

After obtaining the temporal evolution of O_3, NO_x and HCHO, relative concentration sensitivities of these species to different CB6 mechanisms were computed to reveal the dependence of these species on each reaction of the mechanism and the surface emission. The relative concentration sensitivity $\widetilde{S}_{ij}$ can be expressed as

$$\widetilde{S}_{ij} = \frac{\partial \ln c_i}{\partial \ln k_j} = \frac{k_j}{c_i}\frac{\partial c_i}{\partial k_j} = \frac{k_j}{c_i} S_{ij}, \tag{2}$$

which shows the importance of the j-th reaction for the concentration change of the i-th chemical species. In Eq. (2), c_i is the concentration of the i-th chemical species, and k_j denotes the rate constant of the j-th reaction. $S_{ij} = \partial c_i / \partial k_j$ is the absolute concentration sensitivity, and the unit of S_{ij} depends on the order of the j-th reaction. In order to compare the sensitivity coefficients belonging to different reactions, S_{ij} is normalized by being multiplied with k_j/c_i so that a dimensionless sensitivity coefficient, $\widetilde{S}_{ij}$, is obtained. The relative concentration sensitivity $\widetilde{S}_{ij}$ thus represents the percentage change in the i-th species concentration due to a small perturbation in the rate of the j-th reaction. The evaluation of the concentration sensitivity is helpful for discovering the interdependence between the solution of Eq. (1) and input parameters of the model such as the reaction rate constants and the intensity of the surface emission.

The reaction rate constants of the mechanisms were taken from IUPAC database (Atkinson et al., 2004, 2006, 2007, 2008; Crowley et al., 2010; Ammann et al., 2013) and NASA/JPL database (Sander et al., 2006), and a constant temperature 298 K was assumed for the calculation of the reaction rates. Photolytic reaction rates were estimated by using TUV (Tropospheric Ultraviolet and Visible) radiation model (Madronich and Flocke, 1997, 1999), assuming a 300 Dobson overhead ozone column and a 1 km measuring height. Data of cross section and quantum yield for each photolyzed species were taken from CMAQ

https://doi.org/10.5194/acp-2020-1295
Preprint. Discussion started: 15 March 2021


Atmospheric Chemistry and Physics Discussions

model version 5.3 (Byun and Schere, 2006). When the local time resides between 4:30 (sunrise) and 19:30 (sunset), the photolytic reaction rates vary with the solar zenith angle (SZA), while the photolytic reactions are switched off if the local time is out of this range.

In the following section, computational results are presented and discussed.

3 Results and Discussions

We first show the temporal evolution of O_3, NO_x and HCHO obtained by using CB6r1, CB6r2, and CB6r3 under the given initial urban condition, without adding the surface emission. The discrepancies between the results using different mechanisms are also analyzed. Then the concentration sensitivities of the focused species (O_3, NO_x and HCHO) to different CB6 mechanisms are displayed, to indicate the internal difference between these mechanisms. Later on, results with the implementation of the surface emissions are shown. By doing that, the dependence of different CB6 mechanisms on the surface emission under a typical heavily polluted condition can be compared and investigated.

3.1 Temporal evolution of O_3, NO_x and HCHO (no emissions)

Figure 1 shows the temporal profiles of O_3, NO_x and HCHO predicted by CB6r1, CB6r2 and CB6r3, when the surface emission is turned off. It is seen that under this condition, ozone profiles simulated by these three mechanisms show a notable deviation (see Fig. 1a). The ozone predicted by CB6r1 is the highest, while the value predicted by CB6r3 is the lowest under the same initial condition. Because in this scenario the surface emission is not included, the discrepancy between these predictions reflects different capabilities of these mechanisms in converting the initial concentrations into the change of the species. Figure 1(a) shows that at the beginning of the simulation (before day 2), CB6r1 and CB6r2 behave similarly, while CB6r3 predicts a lower value. However, as the reaction proceeds (after day 2), CB6r2 starts to predict a lower ozone than CB6r1, and the simulated profile of CB6r2 approaches to that obtained by CB6r3. In contrast, the ozone predicted by CB6r1 keeps higher than those predicted by CB6r2 and CB6r3. During the end of the 7-day simulation, the ratio between the daily averaged ozone predicted by CB6r1, CB6r2 and CB6r3 over the 7-th day is 1.08:1.02:1. It was found that the ozone predicted by CB6r2 is approximately 2% higher than that predicted by CB6r3. Because the modification in CB6r3 about the temperature dependence gives a same yield of alkyl nitrates under a room temperature (298 K) as that in CB6r2 (Emery et al., 2015), the discrepancy between the ozone predictions obtained by CB6r2 and CB6r3 in this scenario must be caused by other updates in CB6r3. However, it should also be noted that the deviation between the simulations of CB6r2 and CB6r3 becomes smaller when the end of the simulation approaches (see Fig. 1a).

For NO_x simulations, Fig. 1(b) shows that these three mechanisms give almost identical results during the end of the computation. At the beginning of the simulation, NO_x declines rapidly from the initial value (70 ppb) to less than 10 ppb, due to the conversion to PAN (peroxyacetyl nitrate) and HNO_3. At the end of the simulation, the mixing ratio of NO_x becomes lower than 1 ppb. The major nitrogen containing compound during this time period is HNO_3, as PAN is thermally decomposed and photolyzed during the daytime. However, it should be noted that the difference in the predicted NO_x using different mechanisms

https://doi.org/10.5194/acp-2020-1295
Preprint. Discussion started: 15 March 2021


Atmospheric Chemistry and Physics Discussions

may become larger when the surface emission is added to the model due to different capability in transforming emissions into the change of the species for each mechanism.

With respect to HCHO predictions, it is seen in Fig. 1(c) that the deviation between the results of these three mechanisms is more pronounced at the start stage of the simulation. During this time period, CB6r1 predicts a higher HCHO than the other two mechanisms. However, at the end of the simulation, these three mechanisms give a similar HCHO. In model simulations, usually a spin-up process is used to minimize the uncertainty induced by the implementation of an inaccurate initial condition. Based on our results, we found that if HCHO is focused, the spin-up process is also capable of reducing the discrepancy between the HCHO predictions by different CB6 mechanisms, when the surface emission can be neglected.

In summary, we found that when the surface emission is excluded, the ozone concentration predicted by CB6r1 is always higher than that obtained by using CB6r2 or CB6r3. When the end of the simulation approaches, ozone simulated by CB6r1 is approximately 8% larger than that by CB6r3. In contrast to that, after a 7-day computation, the NO_x levels obtained by using these three CB6 mechanisms are almost identical. With respect to HCHO simulations, the discrepancy between the results obtained by CB6r1 and the other two CB6 mechanisms is more pronounced at the beginning of the simulation. However, when the end of the simulation comes, the discrepancy tends to disappear.

3.2 Concentration sensitivity analysis of different CB6 mechanisms (no emissions)

We then conducted a concentration sensitivity analysis on different CB6 mechanisms, and from these results we were able to identify the relative importance of each reaction in these mechanisms for the change of the focused species, and discover the reasons causing the discrepancy between the simulation results of different CB6 mechanisms.

The ozone sensitivity to the CB6r3 mechanism averaged over the last day of the computation is shown in Fig. 2. A positive sensitivity means that an increase of the reaction rate would accelerate the formation of O_3, while a negative value denotes a decline of O_3 when the reaction rate increases. It is seen from Fig. 2 that reactions with large sensitivities mostly possess a reaction number less than 52 (i.e. before Reaction (R52) in the mechanism). Because Reactions (R1)-(R52) in the mechanism represent the inorganic chemistry while reactions after (R52) are mostly VOC-involved reactions (see Tab. A1 in the appendix), it demonstrates an important role of the inorganic chemistry in this simulation, possibly due to the high initial value of NO_x and the omission of VOC emissions in this scenario. From the sensitivity analysis of CB6r3 shown in Fig. 2, we were also able to figure out the most important reactions for the change of ozone, which can be divided into two groups. The first reaction group includes Reactions (R1) $NO_2 + h\nu \rightarrow NO + O$, (R3) $O_3 + NO \rightarrow NO_2$, (R25) $HO_2 + NO \rightarrow OH + NO_2$, (R26) $NO_2 + O_3 \rightarrow NO_3$, (R45) $NO_2 + OH \rightarrow HNO_3$ and (R46) $HNO_3 + OH \rightarrow NO_3$, which are reactions for the inter-conversion of NO_x and the recycling of HNO_3. It demonstrates the significance of reactive nitrogen oxides in determining the final ozone level. The other important reaction group includes (R9) $O_3 + h\nu \rightarrow O(^1D)$, (R10) $O(^1D) + M \rightarrow O + M$, (R11) $O(^1D) + H_2O \rightarrow 2OH$, (R12) $O_3 + OH \rightarrow HO_2$ and (R13) $O_3 + HO_2 \rightarrow OH$. These reactions represent the ozone loss due to the formation of hydrogen oxide radicals (i.e. OH and HO_2). With respect to the other reactions in the mechanism, their sensitivities are all smaller than 0.05 (see Figs. 2b, c and d), denoting a minor influence on the change of ozone by these reactions.

https://doi.org/10.5194/acp-2020-1295
Preprint. Discussion started: 15 March 2021

Atmospheric Chemistry and Physics Discussions

We then computed the ozone sensitivities to the other two mechanisms (i.e. CB6r2 and CB6r1). Because these figures are similar to Fig. 2, we show these results in the supplementary material of the manuscript (Figs. S1 and S2). The similarity between these figures also denotes a consistent treatment of the inorganic chemistry and a similar lumping technique of VOCs in these CB6 mechanisms. By comparing Fig. S1 with Fig. 2, we found that the averaged ozone sensitivity to CB6r2 over the last day is almost identical to the sensitivity to CB6r3, thus leading to a similar ozone prediction by these two mechanisms, which has been shown before (see Fig. 1a). There are two major differences in the ozone sensitivities to CB6r2 and CB6r3. One is that CB6r3 improves upon CB6r2 by adding Reactions (R217)-(R220) to include the temperature dependence of the alkyl nitrate formation. Therefore, the sensitivities of these reactions are absent for CB6r2, shown in Fig. S1 of the supplements. However, as mentioned above, under a condition with a 298 K temperature and 1 atm pressure, the formation of the alkyl nitrate in CB6r2 and CB6r3 are equivalent. Thus, the addition of these reactions in the CB6r3 mechanism would not significantly affect the predicted ozone in this scenario. However, at a different temperature, this update in CB6r3 may bring a large change in O_3, indicated by the relatively large sensitivities of O_3 to Reactions (R219) $\mathrm{XPAR} \rightarrow \mathrm{XO2N} + \mathrm{RO2}$ and (R220) $\mathrm{XPAR} \rightarrow 0.13\mathrm{ALDX} + 0.87\mathrm{ROR} + 0.13\mathrm{XO2H} + 0.87\mathrm{XO2} + \mathrm{RO2} - 0.13\mathrm{PAR}$, shown in Fig. 2. Aside from this modification, another major difference between CB6r2 and CB6r3 is Reaction (R158). In CB6r2, it has a form of $\mathrm{ISPD} + \mathrm{OH} \rightarrow 0.06\mathrm{XO2N} + 0.52\mathrm{XO2} + 0.24\mathrm{XO2H} + 0.15\mathrm{MGLY} + 0.27\mathrm{MEO2} + 0.12\mathrm{GLY} + 0.35\mathrm{GLYD} + 0.23\mathrm{C2O3} + 0.12\mathrm{CXO3} + 0.24\mathrm{PAR} + 0.26\mathrm{ACET} + 0.20\mathrm{CO} + 0.14\mathrm{HO_2} + 1.09\mathrm{RO2}$. In contrast, in CB6r3, it is formulated as $\mathrm{ISPD} + \mathrm{OH} \rightarrow 0.02\mathrm{XO2N} + 0.52\mathrm{XO2} + 0.12\mathrm{MGLY} + 0.12\mathrm{MEO2} + 0.27\mathrm{GLYD} + 0.27\mathrm{C2O3} + 0.46\mathrm{OPO3} + 0.12\mathrm{PAR} + 0.14\mathrm{ACET} + 0.14\mathrm{CO} + 0.14\mathrm{HO_2} + 0.66\mathrm{RO2}$, so that the products are updated. Because in CB6r2, Reaction (R158) produces XO2H, which is an operator representing the conversion from NO to NO_2. In contrast to that, Reaction (R158) in CB6r3 does not produce XO2H. As a result, the NO to NO_2 conversion in CB6r2 is accelerated, thus enhancing the formation of O_3. Due to this modification, the ozone sensitivity belonging to this reaction shifts from a positive value in CB6r2 (see Fig. S1 of the supplements) to a negative value in CB6r3 (see Fig. 2). It was estimated that this update in Reaction (R158) between CB6r3 and CB6r2 is mostly responsible for the 2% discrepancy in the simulated ozone, which has been shown in Fig. 1(a).

We then tried to figure out reactions causing the higher ozone prediction of CB6r1. From a comparison between Fig. S1 and Fig. S2 in the supplementary material, we found the modification of Reaction (R66) about the sink of CXO3 heavily responsible for the higher ozone prediction of CB6r1. CXO3 represents acylperoxy radicals with three and higher carbons, and is able to oxidize NO and thus form ozone. In CB6r1, the form of Reaction (R66) is as follows, $\mathrm{CXO3} + \mathrm{RO2} \rightarrow \mathrm{CXO3}$, while in CB6r2, the form is $\mathrm{CXO3} + \mathrm{RO2} \rightarrow 0.8\mathrm{ALD2} + 0.8\mathrm{XO2H} + 0.8\mathrm{RO2}$. In CB6r1, the total amount of CXO3 is unaltered through Reaction (R66), thus leading to a negligible ozone sensitivity to (R66). However, the update of Reaction (R66) in CB6r2 causes this reaction to be a major sink of CXO3 in the mechanism. As a result, the significance of Reaction (R66) increases in CB6r2. Moreover, due to the enhanced importance of Reaction (R66), it was found in CB6r2 that the significance of many other CXO3 related reactions, (R62) $\mathrm{CXO3} + \mathrm{NO_2} \rightarrow \mathrm{PANX}$, (R63) $\mathrm{PANX} \rightarrow \mathrm{NO_2} + \mathrm{CXO3}$, (R65) $\mathrm{CXO3} + \mathrm{HO_2} \rightarrow 0.41\mathrm{PACD} + 0.15\mathrm{AACD} + 0.15\mathrm{O_3} + 0.44\mathrm{ALD2} + 0.44\mathrm{XO2H} + 0.44\mathrm{RO2} + 0.44\mathrm{OH}$ and (R67) $\mathrm{CXO3} + \mathrm{CXO3} \rightarrow 2\mathrm{ALD2} + 2\mathrm{XO2H} + 2\mathrm{RO2}$, drops, from a moderate value in CB6r1 to a small value in CB6r2. The formation of ozone in CB6r2 is thus getting suppressed due to the additional consumption of CXO3 through Reaction (R66). This finding also denotes an important role of CXO3 in

https://doi.org/10.5194/acp-2020-1295
Preprint. Discussion started: 15 March 2021

Atmospheric Chemistry and Physics Discussions

determining ozone in the CB6 mechanisms. Thus, more attention should be paid to CXO3 related reactions in future mechanism developments. The significance of CXO3 in the mechanism for the conversion of NO to NO_2 and the formation of ozone has also been identified by Luecken et al. (2008) in a model study on the behavior of three chemical mechanisms. Aside from the change of Reaction (R66), we also found two reactions in CB6r2, (R213) $\mathrm{OPAN+OH \rightarrow 0.5NO_2+0.5GLY+CO+0.5NTR2}$ and (R214) $\mathrm{PANX + OH \rightarrow NO_2 + ALD2}$, absent in CB6r1. Because Reactions (R213) and (R214) consume OH, which is essential for the recycling of HNO_3, missing these two reactions in CB6r1 would cause a higher OH prediction and thus an enhanced ozone formation in CB6r1. In addition, the absent of NTR2 (multi-functional nitrates) in CB6r1 also contributes to the higher ozone prediction of CB6r1. It is because that NTR2 in CB6r2 participates in the reaction $\mathrm{NTR2 + H_2O_{(aerosol)} \rightarrow HNO_3}$, which is a loss pathway for the reactive nitrogen oxides, thus leading to a lower ozone prediction of CB6r2 than that of CB6r1. It is also interesting to note that the form of Reaction (R158) in CB6r1 is also different from CB6r2. However, the sensitivity belonging to this reaction in CB6r1 is similar to that in CB6r2, meaning that the modification in Reaction (R158) between CB6r1 and CB6r2 is not the major reason for the different ozone predictions using these two mechanisms.

From the discussions above, it was found that in different versions of the CB6 mechanism, Reaction (R158) has a different form (see Tab. A1), thus playing a different role in the formation and consumption of ozone. We thus displayed the temporal evolutions of the ozone sensitivity to Reaction (R158) for different CB6 mechanisms (see Fig. 3). It can be seen that in CB6r1 and CB6r2, Reaction (R158) always has a positive sensitivity, while in CB6r3 it possesses a negative value. The deviation in the ozone sensitivity to Reaction (R158) between CB6r2 and CB6r3 is more pronounced at the beginning of the simulation. As the simulation proceeds, the deviation becomes smaller. This temporal change of the ozone sensitivity to Reaction (R158) is in agreement with the time-varying changes of the predicted ozone shown in Fig. 1. It means that Reaction (R158) is possibly the major reason causing the difference in the predicted ozone between CB6r2 and CB6r3. In contrast, the temporal behavior of the (R158) sensitivity for CB6r1 and CB6r2 are similar (see Fig. 3), especially during the end of the simulation. Thus, the update of Reaction (R158) between CB6r1 and CB6r2 is not responsible for the different ozone predictions by these two mechanisms.

The NO_x sensitivity to the CB6r3 mechanism is displayed in Fig. 4. It is seen that in CB6r3, reactions for the recycling of HNO_3: (R45) $\mathrm{NO_2 + OH \rightarrow HNO_3}$, (R46) $\mathrm{HNO_3 + OH \rightarrow NO_3}$, (R47) $\mathrm{HNO_3 + h\nu \rightarrow OH + NO_2}$ and (R26) $\mathrm{NO_2 + O_3 \rightarrow NO_3}$ are the most determining reactions for the change of NO_x. It is because that HNO_3 is the largest sink of the reactive nitrogen oxides, thus controlling the final value of NO_x. Regarding to the other reactions in the mechanism, their sensitivities are much smaller, thus bringing a negligible influence on the change of NO_x. The sensitivities of NO_x to the other two CB6 mechanisms, CB6r2 and CB6r1, are shown in Figs. S3 and S4 of the supplementary material, respectively. It was found that the sensitivities of NO_x to these two CB6 mechanisms (i.e. CB6r2 and CB6r1) are strongly similar to the sensitivity to CB6r3. The largest change in the NO_x sensitivity between CB6r3 and the other two mechanisms is the addition of the reactions representing the temperature dependence of alkyl nitrate formation, i.e. Reactions (R217)-(R220) in Fig. 4. However, as mentioned above, the scheme for the temperature dependence in CB6r3 is equivalent to that in CB6r2 under the situation used in this study. Thus, adding these reactions into CB6r3 would not exert a significant influence on the change of NO_x. But the moderate sensitivity coefficients belonging to Reactions (R219) and (R220) shown in Fig. 4 denote that under a different temperature condition, the change of NO_x brought about by this update might be larger. Apart from this change, other reactions that largely

https://doi.org/10.5194/acp-2020-1295
Preprint. Discussion started: 15 March 2021


Atmospheric Chemistry and Physics Discussions

modified between different CB6 mechanisms possess a small sensitivity coefficient. Thus, the implementation of different CB6 mechanisms in the present model would not significantly influence the predicted NO_x.

At last, for the HCHO sensitivity, it is seen in Fig. 5 that in CB6r3, the major HCHO decay pathways include Reactions (R96) $\mathrm{HCHO} + \mathrm{OH} \rightarrow \mathrm{HO_2} + \mathrm{CO}$, (R97) $\mathrm{HCHO} + h\nu \rightarrow 2\mathrm{HO_2} + \mathrm{CO}$ and (R98) $\mathrm{HCHO} + h\nu \rightarrow \mathrm{H_2} + \mathrm{CO}$. In contrast, the largest HCHO formation pathway is found as Reaction (R124) $\mathrm{CH_4} + \mathrm{OH} \rightarrow \mathrm{MEO2} + \mathrm{RO2}$. It is due to the large amount of CH_4 in the initial condition, which is the major source of HCHO through its oxidation. By comparing the HCHO sensitivity to CB6r3 shown in Fig. 5 with the HCHO sensitivities to CB6r2 (Fig. S5 of the supplements) and CB6r1 (Fig. S6 of the supplements), it was found that the largest change in the HCHO sensitivity between CB6r3 and CB6r2 is again the addition of reactions representing the temperature dependence in CB6r3. However, similar to the findings discussed above, the prediction of HCHO by CB6r3 is not heavily affected by the addition of these reactions under a standard condition and thus is similar to that by CB6r2. Most interestingly, different from the situations in simulating ozone and NO_x, it was found in Fig. 5 that the reactions representing the temperature dependence (i.e. Reactions (R217)-(R220)) possess relatively small HCHO sensitivities (<0.01). Thus, it can be expected that even under a different temperature condition, the influence on HCHO caused by the change of temperature is also possibly small. With respect to the HCHO sensitivity to CB6r1, it was found that the most determining reactions for HCHO are all kept unchanged. On the contrary, reactions that largely modified between different versions of the mechanism mostly possess small sensitivity coefficients. As a result, CB6r1 also gives a similar HCHO prediction in this scenario.

In general, the sensitivity analysis shows that when the surface emission is neglected, the update in CB6r2 and CB6r3 compared with CB6r1 that can strongly affect the ozone prediction is the change in the sink of CXO3, i.e. Reaction (R66). Because of this modification, the significance of many CXO3 related reactions also changes, causing a lower ozone prediction of CB6r2 and CB6r3 than that of CB6r1. On the contrary, the ozone sensitivities to CB6r2 and CB6r3 are approximately the same, thus leading to a similar O_3 prediction. With respect to NO_x and HCHO, reactions that largely modified between different versions of the CB6 mechanism mostly have small sensitivities so that the updates in these CB6 mechanisms exert a negligible impact on the prediction of NO_x and HCHO in this scenario. However, under a different temperature condition, the prediction of NO_x by CB6r3 might be largely different from those predicted by CB6r2 and CB6r1, indicated by the moderate values of the sensitivities belonging to the temperature dependent reactions in CB6r3.

3.3 Temporal evolution of ozone, NO_x and HCHO (with emissions)

The temporal profiles of O_3, NO_x and HCHO in the scenario including the surface emission is shown in Fig. 6. The intensity of the surface emission for each species is given in Tab. 1. It is seen from Fig. 6(a) that after adding the surface emission, ozone increases steadily from the beginning of the simulation. The ozone level at the end of the 7-day simulation is within a range of 250-350 ppb, much higher than that in the scenario without the surface emission (∼200-220 ppb). By comparing ozone profiles obtained by using different CB6 mechanisms in Fig. 6(a), we found the ozone predictions by CB6r2 and CB6r3 approximately the same, while CB6r1 predicts a much higher value. It was calculated that the averaged ozone over the 7-th day predicted by CB6r1 is approximately 20% higher than that predicted by CB6r2 or CB6r3. Thus, after adding the surface

https://doi.org/10.5194/acp-2020-1295
Preprint. Discussion started: 15 March 2021


Atmospheric Chemistry and Physics Discussions

emission, the deviation in the predicted ozone between CB6r1 and the other two CB6 mechanisms is enlarged, compared with that in the no-emission scenario. It demonstrates that the CB6r1 mechanism has a stronger transformation ability in converting the surface emission into the change of ozone than the other two mechanisms. As a result, simulations using CB6r1 would yield a much higher ozone than that using CB6r2 or CB6r3, even though a same intensity of the surface emission is applied. In a previous regional modeling of the air quality across the continental US (Ruiz Hildebrandt and Yarwood, 2013), it was reported that CB6r1 predicts a higher ozone than CB6r2. Thus, the results of the present study are consistent with the conclusions of Ruiz Hildebrandt and Yarwood (2013).

The change of NO_x with time is displayed in Fig. 6(b). It shows that NO_x declines rapidly from the relatively high initial value (70 ppb) to a stable level, 3-5 ppb. This final value range is also much higher than that in the no-emission scenario (<1 ppb). An obvious diurnal variation of NO_x is exhibited, and two peaks were found in the early morning and the late afternoon of each day. Figure 6(b) also shows that CB6r2 and CB6r3 give similar NO_x predictions, while CB6r1 behaves differently. CB6r1 predicts a higher NO_x than CB6r2 and CB6r3 during the daytime, but in the nighttime it gives a lower NO_x. We figured out the reason for this discrepancy is that in CB6r1, Reaction (R66) has a form of $\mathrm{CXO3} + \mathrm{RO2} \rightarrow \mathrm{CXO3}$, which has been discussed above. As a result, the amount of CXO3 is unaltered through Reaction (R66) in CB6r1. Then CXO3 in CB6r1 turns to be more involved in reactions forming PANX (peroxyacyl nitrate with three and higher carbons). This trend is also confirmed by the relatively higher amount of PANX predicted by CB6r1 than those predicted by CB6r2 and CB6r3 (not shown here). As a result, during the nighttime, an additional amount of NO_x in CB6r1 is converted to PANX, causing a lower prediction of NO_x in CB6r1. In contrast, when the sun rises, the photolysis of PANX leads to a more rapid increase of NO_x in CB6r1, compared with that in CB6r2 and CB6r3.

With respect to HCHO, we found that due to the inclusion of the surface emission, the level of HCHO keeps increasing when the simulation proceeds. The emitted species that are responsible for the enhancement of HCHO will be investigated in a later context. The temporal change of HCHO shows a strong diurnal variation, in which it peaks at the midnight and roughs at noon of every day. The predicted HCHO profiles using CB6r2 and CB6r3 are found almost identical. In a box model study of Marvin et al. (2017), they also found that using CB6r3 causes a negligible impact (<1%) on the simulated HCHO compared to using CB6r2, which is consistent with the findings of the present study. In contrast to that, CB6r1 consistently yields a higher value of HCHO. At the 7-th day of the simulation, the peak value of HCHO obtained by CB6r1 is around 55 ppb, while the lowest value is approximately 32 ppb. The deviation between the HCHO concentrations predicted by CB6r1 and the other two mechanisms is approximately 10 ppb. These values are all much higher than those in the no-emission simulation (see Fig. 1c), due to the inclusion of the surface emission.

In summary, due to the inclusion of the surface emission, a strong enhancement of the predicted O_3, NO_x and HCHO was found, compared with the no-emission scenario. Moreover, simulated results of CB6r2 and CB6r3 are almost identical, while CB6r1 consistently gives higher values of O_3 and HCHO than the other two mechanisms. The most special finding in this scenario is the prediction of NO_x, as the daytime level of NO_x predicted by CB6r1 is higher than that predicted by CB6r2 and CB6r3, but the nighttime NO_x given by CB6r1 is lower than that given by the other two mechanisms. It is because that NO_x

https://doi.org/10.5194/acp-2020-1295
Preprint. Discussion started: 15 March 2021


Atmospheric Chemistry and Physics Discussions

in CB6r1 participate more frequently in the formation of PANX, leading to a larger NO_x consumption in the nighttime and a more rapid NO_x formation in the daytime.

3.4 Concentration sensitivity analysis of different CB6 mechanisms (with emissions)

The concentration sensitivity analysis was applied on these CB6 mechanisms again, after adding the surface emission. Figure 7 shows the ozone sensitivity to the CB6r3 mechanism. Note that Reactions (R222)-(R234) in Fig. 7 represent the sensitivities to the surface emission. From a global view, it can be found that after adding the surface emission, the importance of most reactions in the mechanism increases, compared with the no-emission case. Reactions that the significance changes the most are (1) NO_x related reactions: (R1) $NO_2 + h\nu \rightarrow NO + O$ and (R3) $O_3 + NO \rightarrow NO_2$; (2) CXO3 related reactions: (R61) $CXO3 + NO \rightarrow NO_2 + ALD2 + XO2H + RO2$, (R75) $XO2H + NO \rightarrow NO_2 + HO_2$, (R76) $XO2H + HO_2 \rightarrow ROOH$ and (R77) $XO2H + C2O3 \rightarrow 0.8HO_2 + 0.8MEO2 + 0.2AACD + 0.8RO2$; (3) isoprene related reactions: (R149) $ISOP + OH \rightarrow ISO2 + RO2$ and (R157) $ISOP + NO_3 \rightarrow 0.35NO_2 + 0.65NTR2 + 0.64XO2H + 0.33XO2 + 0.03XO2N + RO2 + 0.35HCHO + 0.35ISPD$. In addition, Fig. 7(d) shows that the surface emission exerts a strong influence on the change of ozone, reflected by the relatively large ozone sensitivities to Reactions (R222)-(R234). It can be seen in Fig. 7 that the ozone sensitivities to the surface emission are comparable to that belonging to the NO_x related reactions (i.e. (R1) and (R3)).

Among the surface emissions, the most influential emitted species for the change of O_3 is NO (see Fig. 7d). It is not surprising as the oxidation of of the emitted NO by the hydroperoxy radical and methylperoxy radicals would form O_3. Aside from this, the release of NO_2 would also increase the O_3 level, through its photolytic decomposition. In contrast to the NO_x emissions, the increase of VOC emissions in this scenario would decrease the formation of O_3, which is indicated in Fig. 7(d) by the negative ozone sensitivities to the VOC emissions. Moreover, it was found that the ozone sensitivity to the emissions of NO_x is larger than that to the VOC emissions. This trend has also been revealed by Luecken et al. (2018), showing that the dependence of ozone on NO_x is approximately three times as heavy as that on hydrocarbons in their model studies. In the present study, the most influential VOC for the change of O_3 is found as ISOP (isoprene). Isoprene can react rapidly with OH and NO_3, which substantially contributes to the formation and consumption of ozone. Thus, more attention should be paid to the isoprene emission applied in air quality models in order to achieve a more accurate ozone prediction. In previous studies, it was shown that different biogenic emission models (e.g. MEGAN and BEIS) may yield different isoprene emission estimates (Bash et al., 2016; Zhang et al., 2017b). Thus, the choice of the biogenic emission model in the settings of the air quality model would strongly influence the modeled ozone, according to the findings of the present study. Moreover, an enhancement of the emissions of terminal olefins (OLE), toluene (TOL), xylene and other polyalkyl aromatics (XYLMN) would also reduce the ozone level. From the response of the ozone concentration to the surface emission, we concluded that in this scenario, an emission control of NO_x especially NO is effective in reducing O_3, while an emission control of VOCs leads to an increase of ozone, when CB6r3 is implemented.

The ozone sensitivities to the reactions of CB6r2 and CB6r1 as well as the surface emissions are shown in Figs. S7 and S8 of the supplementary material. First, by comparing Fig. 7 with Fig. S7 in the supplements, we found that with the inclusion of the surface emission, the ozone sensitivities to CB6r3 and CB6r2 are approximately the same. Although the update of

https://doi.org/10.5194/acp-2020-1295
Preprint. Discussion started: 15 March 2021


Atmospheric Chemistry and Physics Discussions

Reaction (R158) mentioned above between CB6r2 and CB6r3 still causes a sensitivity shift from a positive value to a negative value, the impact caused by this sensitivity shift is negligible compared with the influence brought about by the inclusion of the surface emission. As a result, under this condition, O_3 predicted by CB6r3 is approximately equal to that predicted by CB6r2, which has been displayed in Fig 6(a). For the CB6r1 mechanism, the ozone sensitivity displayed in Fig. S8 of the supplements shows a remarkable difference, especially in the dependence of O_3 on the surface emission. It was found that the dependence of O_3 on the emission of isoprene is much weaker in CB6r1 than that in CB6r2 and CB6r3 (see the sensitivity to Reaction (R233) in Fig. S8 of the supplements). Thus, in CB6r1, the emitted VOC that O_3 depends on the most becomes OLE (terminal olefins) instead of ISOP (isoprene). As a result, the O_3 destruction caused by the isoprene emission is significantly suppressed in CB6r1. Moreover, the importance of isoprene related reactions, such as Reactions (R149) $\mathrm{ISOP} + \mathrm{OH} \rightarrow \mathrm{ISO2} + \mathrm{RO2}$ and (R157) $\mathrm{ISOP} + \mathrm{NO_3} \rightarrow 0.35\mathrm{NO_2} + 0.65\mathrm{NTR2} + 0.64\mathrm{XO2H} + 0.33\mathrm{XO2} + 0.03\mathrm{XO2N} + \mathrm{RO2} + 0.35\mathrm{HCHO} + 0.35\mathrm{ISPD}$, also becomes weaker in CB6r1 than in CB6r2 and CB6r3. Therefore, after adding the surface emission, due to the less dependence of O_3 on the emitted isoprene, the O_3 level predicted by CB6r1 is higher than that predicted by CB6r2 and CB6r3, which has been shown in Fig 6(a). In the no-emission case shown before, we found the modification in Reaction (R66) about the sink of CXO_3 to be the major reason causing the difference between the simulation results of CB6r1 and CB6r2/CB6r3. However, it can be seen in Fig. S8 that after adding the surface emission, the ozone sensitivity to Reaction (R66) is 1-2 orders smaller than the sensitivity to the surface emission. Therefore, the discrepancy in the predicted ozone between different CB6 mechanisms is mostly caused by the change of the O_3 dependence on the surface emission, especially the release of isoprene.

The sensitivity of NO_x to the reactions of the CB6r3 mechanism and the surface emission is displayed in Fig. 8. After adding the surface emission, the most dominant factor for the change of NO_x is the emission of NO. Moreover, the significance of Reactions (R1) $\mathrm{NO_2} + h\nu \rightarrow \mathrm{NO} + \mathrm{O}$, (R3) $\mathrm{O_3} + \mathrm{NO} \rightarrow \mathrm{NO_2}$, (R25) $\mathrm{HO_2} + \mathrm{NO} \rightarrow \mathrm{OH} + \mathrm{NO_2}$ and (R26) $\mathrm{NO_2} + \mathrm{O_3} \rightarrow \mathrm{NO_3}$, which represent the inter-conversion of reactive nitrogen oxides, increases, compared with that in the no-emission scenario. In contrast to that, the NO_x sensitivity to the HNO_3 related reactions (R45) $\mathrm{NO_2} + \mathrm{OH} \rightarrow \mathrm{HNO_3}$, (R46) $\mathrm{HNO_3} + \mathrm{OH} \rightarrow \mathrm{NO_3}$ and (R47) $\mathrm{HNO_3} + h\nu \rightarrow \mathrm{OH} + \mathrm{NO_2}$ decreases. It represents that after including the surface emission, the amount of NO_x becomes abundant, so that the loss of NO_x caused by the HNO_3 formation is no longer a limited factor for the change of NO_x under this situation.

As mentioned above, in CB6r3, the emitted species that NO_x depends on the most is NO (see Fig. 8d), which is natural as the direct emission of NO would strongly increase NO_x. The release of NO_2 also elevates the NO_x level predicted by CB6r3. In contrast to that, the release of VOCs tends to suppress the formation of NO_x, denoted by the negative sensitivities to VOC emissions. The most influential VOC for the change of NO_x is also the species ISOP (isoprene), identifying the important role of isoprene in the CB6r3 mechanism.

From a comparison between the NO_x sensitivities to CB6r2 (shown in Fig. S9 of the supplements) and CB6r3 (see Fig. 8), again we found that the NO_x sensitivity to CB6r2 is almost identical to that to CB6r3, thus leading to a similar prediction of NO_x by these two mechanisms. However, for CB6r1 (see Fig. S10 of the supplements), similar to the findings in the sensitivity analysis of O_3, the NO_x mixing ratio predicted by CB6r1 depends less on the surface emission of isoprene. Aside from that, it was found in CB6r1 that the dependence of NO_x on all the emissions becomes weaker than that in CB6r2 and CB6r3. It means

https://doi.org/10.5194/acp-2020-1295
Preprint. Discussion started: 15 March 2021

Atmospheric Chemistry and Physics Discussions

that in the CB6r1 mechanism, the influence caused by the addition of the surface emission is smaller, and the change of NO_x is more associated with the local chemical reactions such as the PANX formation. This enhanced NO_x dependence on the local chemistry in CB6r1 is also indicated by the increasing sensitivities of many reactions in the mechanism, such as the PANX formation and consumption reactions, i.e. (R62) $\mathrm{CXO3} + \mathrm{NO_2} \rightarrow \mathrm{PANX}$ and (R63) $\mathrm{PANX} \rightarrow \mathrm{NO_2} + \mathrm{CXO3}$ (see Fig. S10 of the supplements), compared with that in CB6r3 and CB6r2 (Fig. 8 and Fig. S9 of the supplementary material). It thus leads to an enhanced formation of PANX and a stronger diurnal change in the NO_x concentration in CB6r1, which has been displayed in Fig. 6(c).

At last, we focused on the averaged sensitivities of HCHO to these three different CB6 mechanisms. Figure 9 shows the HCHO sensitivities to the reactions and the surface emission for the CB6r3 mechanism. It was found that reactions that play an important role in the change of HCHO include (R96) $\mathrm{HCHO} + \mathrm{OH} \rightarrow \mathrm{HO_2} + \mathrm{CO}$, (R97) $\mathrm{HCHO} + h\nu \rightarrow 2\mathrm{HO_2} + \mathrm{CO}$, and (R98) $\mathrm{HCHO} + h\nu \rightarrow \mathrm{CO}$, which are reactions consuming HCHO. These important HCHO decay reactions are the same to those in the no-emission case. However, Reaction (R124) $\mathrm{CH_4} + \mathrm{OH} \rightarrow \mathrm{MEO2} + \mathrm{RO2}$ that used to strongly promote the formation of HCHO in the no-emission scenario no longer possesses a large sensitivity. It denotes a decreased importance of the initial CH_4 in the formation of HCHO after adding the surface emission in the model. Instead, the release of VOCs would significantly promote the formation of HCHO.

From the dependence of HCHO on the surface emission displayed in Fig. 9(d), we found that an increase in the emission intensity of VOCs especially isoprene and terminal olefins would significantly enhance the HCHO formation, and the influence caused by the emissions of isoprene and terminal olefins is approximately equal, indicated by the similar sensitivities to these two emissions. This strong influence of the emissions of isoprene and other olefins on the change of HCHO has also been identified in many previous studies (Luecken et al., 2006, 2008; Wolfe et al., 2016; Marvin et al., 2017). Moreover, in the present study, we found that the increase of NO_x leads to a decline of HCHO. It is because that the release of NO_x would cause an elevated amount of OH, through the oxidation of NO and the formation of ozone. As Reaction (R96) $\mathrm{HCHO} + \mathrm{OH} \rightarrow \mathrm{HO_2} + \mathrm{CO}$ is a major pathway for the destruction of HCHO, the increase of OH would reduce HCHO, thus leading to a negative dependence of HCHO on the release of NO_x. It was also found in this study that HCHO is more sensitive to VOCs than NO_x, which is in accordance with the conclusions achieved in the previous sensitivity study of HCHO to precursor species (Luecken et al., 2018). The reason is that HCHO can be formed under both NO_x-rich and NO_x-poor conditions, resulting in a weaker dependence of HCHO on the NO_x emissions.

In a previous modeling study conducted by Luecken et al. (2019) using CB6r3, they found an underestimation of HCHO in a comparison with observations across the US. Luecken et al. (2019) suggested that the underestimation of HCHO might be caused by the uncertainties in biogenic emissions including direct HCHO emissions and other VOC emissions. Based on our findings, we suggested that the underestimation of HCHO might be caused by the underestimation of isoprene and other alkene emissions. In contrast, the direct emission of HCHO may possibly only exert a minor impact on the change of HCHO, according to the sensitivity analysis of CB6r3 in the present study. In the study of Luecken et al. (2019), they also performed a sensitivity test by doubling the isoprene emission, and it was found that the simulated HCHO is elevated due to the enhancement of the isoprene emission. This is also in accordance with our findings in the present study.

https://doi.org/10.5194/acp-2020-1295
Preprint. Discussion started: 15 March 2021


Atmospheric Chemistry and Physics Discussions

By comparing the HCHO sensitivities to CB6r3 (Fig 9) and CB6r2 (Fig. S11 in the supplements), we noticed that the most dominant reactions for the change of HCHO approximately the same in these two mechanisms, thus leading to a similar HCHO prediction by these two mechanisms. However, the sensitivity of HCHO to CB6r1 displayed in Fig. S12 of the supplements shows that in CB6r1, the significance of the isoprene emission is much higher than that in CB6r2 and CB6r3. As a result, a same increment in the isoprene emission would lead to a relatively larger increase in HCHO predicted by CB6r1 relative to that predicted by CB6r2 or CB6r3. This is also the reason for the relatively higher HCHO prediction by CB6r1 shown in Fig. 6. This finding again indicates the importance of revising the isoprene chemistry in future updates to the CB6 mechanism.

In summary, in the situation with the inclusion of the surface emission in the model, we found that the ozone level predicted by CB6r2 and CB6r3 depends heavily on the surface emission especially the release of NO and isoprene. In contrast, the dependence of ozone on the isoprene is weaker in CB6r1. Aside from that, the importance of many isoprene related reactions in CB6r1 decreases, which is shown in the sensitivity analysis. These changes in the ozone sensitivity lead to a higher ozone prediction of CB6r1 relative to that of CB6r2 and CB6r3, even though a same surface emission condition is applied. With respect to the change of NO_x, in CB6r2 and CB6r3, the most influential emissions are also the release of NO and isoprene. However, in CB6r1, the predicted NO_x relies less on the surface emission, and the local chemistry especially the formation of PANX plays a more important role in determining NO_x, leading to a higher NO_x prediction during the daytime and a lower NO_x prediction during the nighttime in CB6r1, respectively. At last, for HCHO, the increase of the NO_x emission would decrease the HCHO predictions of these CB6 mechanisms. In contrast, the enhancement of VOC emissions particularly isoprene and terminal olefins would significantly promote the formation of HCHO. However, the dependence of HCHO on the release of isoprene in CB6r1 is stronger than that in the other two mechanisms, thus leading to a higher prediction of HCHO in CB6r1 under the same emission conditions.

4 Conclusions and Future Work

In the present study, we found that different versions of the CB6 mechanism perform differently in simulating O_3, NO_x and HCHO, although the same initial condition and the same intensity of the surface emission is set up. When the surface emission is turned off, CB6r1 predicts a higher ozone value than the other two mechanisms, and the relative deviation is approximately 8%. The sensitivity analysis suggests that the higher ozone prediction by CB6r1 is mostly caused by the modification of the chemical loss pathways of acylperoxy radicals with three and higher carbons (i.e. species CXO3) in the mechanism. Due to this modification, less CXO3 is consumed in CB6r1 than that in CB6r2 and CB6r3, resulting in a higher ozone prediction by CB6r1. Regarding to NO_x and HCHO, the predictions by these three CB6 mechanisms are similar during the end of the simulation. However, the sensitivity analysis shows that the update in CB6r3 about the temperature dependence of organic nitrate formation might exert a strong influence on the prediction of ozone and NO_x under a different temperature condition, while the impact of the temperature change on HCHO might be minor.

After implementing the surface emissions into the model, we found the simulated levels of O_3, NO_x and HCHO elevated, compared with those in the no-emission scenario. It was also found that the ozone concentration predicted by CB6r2 and CB6r3

https://doi.org/10.5194/acp-2020-1295
Preprint. Discussion started: 15 March 2021

Atmospheric Chemistry and Physics Discussions

depends on the emissions of NO and isoprene the most, while in CB6r1 the dependence of ozone on the isoprene emission is weaker. Because in this simulation, the isoprene emission tends to suppress the ozone formation, ozone predicted by CB6r1 is thus higher than those predicted by CB6r2 and CB6r3 with the same emission intensity. With respect to the NO_x prediction, in CB6r1, NO_x depends more on the local chemistry such as the formation of PANX than that in CB6r2 and CB6r3. As a result, NO_x in CB6r1 is more involved in the formation of reservoirs such as PANX, thus leading to a lower NO_x prediction at nighttime and a higher NO_x prediction at daytime compared with that in CB6r2 and CB6r3. At last, we found that the HCHO predictions of these three CB6 mechanisms rely mostly on the emissions of NO, isoprene and terminal olefins. However, in CB6r1, the association between HCHO and the isoprene emission is stronger, resulting in a higher HCHO prediction relative to that in CB6r2 and CB6r3 with the same isoprene emission.

In the future, we plan to test the behavior of these CB6 mechanisms under different environmental conditions with different surface emission intensities. The influence caused by the varying of the temperature on the concentration change of the focused species, especially for CB6r3 should also be investigated. Moreover, the latest version of the CB6 mechanism, CB6r4 (Emery et al., 2016), should be studied and compared with the three CB6 mechanisms investigated in the present study, particularly in a halogen-rich environment. In addition, the conclusions achieved in this box-model study need to be confirmed in simulations using multi-dimensional air quality models. At present, we are conducting three-dimensional simulations using CMAQ (Byun and Schere, 2006) and CAMx (ENVIRON, 2015) to discover the difference in modeling O_3, NO_x and HCHO by using these different versions of the CB6 mechanism, which is attributed to a future publication.

Code and data availability. The source code of the model and the data of the computational results shown in this article can be acquired upon request from the authors.

Appendix A

Acknowledgements. This work was supported by the National Key R&D Program of China (Grant No. 2017YFC0209801) and the National Natural Science Foundation of China (Grant No. 41375044). The numerical calculations in this paper have been done on the high performance computing system in the High Performance Computing Center, Nanjing University of Information Science & Technology.

Author contributions. Le Cao conceived the idea of the article and wrote the python script for the conversion of the data format. Le Cao also configured and performed the computations. Simeng Li revised the chemical mechanisms and wrote the paper with Le Cao together. Luhang Sun revised the paper and gave valuable suggestions. All the authors listed have read and approved the final manuscript.

https://doi.org/10.5194/acp-2020-1295
Preprint. Discussion started: 15 March 2021

Atmospheric Chemistry and Physics Discussions

Competing interests. The authors declare no conflict of interest.

https://doi.org/10.5194/acp-2020-1295
Preprint. Discussion started: 15 March 2021

Atmospheric Chemistry and Physics Discussions

References

Ammann, M., Cox, R. A., Crowley, J. N., Jenkin, M. E., Mellouki, A., Rossi, M. J., Troe, J., and Wallington, T. J.: Evaluated kinetic and photochemical data for atmospheric chemistry: Volume VI – heterogeneous reactions with liquid substrates, Atmospheric Chemistry and Physics, 13, 8045–8228, https://doi.org/10.5194/acp-13-8045-2013, 2013.

Atkinson, R., Baulch, D. L., Cox, R. A., Crowley, J. N., Hampson, R. F., Hynes, R. G., Jenkin, M. E., Rossi, M. J., and Troe, J.: Evaluated kinetic and photochemical data for atmospheric chemistry: Volume I - gas phase reactions of O_x, HO_x, NO_x and SO_x species, Atmospheric Chemistry and Physics, 4, 1461–1738, https://doi.org/10.5194/acp-4-1461-2004, 2004.

Atkinson, R., Baulch, D. L., Cox, R. A., Crowley, J. N., Hampson, R. F., Hynes, R. G., Jenkin, M. E., Rossi, M. J., Troe, J., and Subcommittee, I.: Evaluated kinetic and photochemical data for atmospheric chemistry: Volume II - gas phase reactions of organic species, Atmospheric Chemistry and Physics, 6, 3625–4055, https://doi.org/10.5194/acp-6-3625-2006, 2006.

Atkinson, R., Baulch, D. L., Cox, R. A., Crowley, J. N., Hampson, R. F., Hynes, R. G., Jenkin, M. E., Rossi, M. J., and Troe, J.: Evaluated kinetic and photochemical data for atmospheric chemistry: Volume III - gas phase reactions of inorganic halogens, Atmospheric Chemistry and Physics, 7, 981–1191, https://doi.org/10.5194/acp-7-981-2007, 2007.

Atkinson, R., Baulch, D. L., Cox, R. A., Crowley, J. N., Hampson, R. F., Hynes, R. G., Jenkin, M. E., Rossi, M. J., Troe, J., and Wallington, T. J.: Evaluated kinetic and photochemical data for atmospheric chemistry: Volume IV – gas phase reactions of organic halogen species, Atmospheric Chemistry and Physics, 8, 4141–4496, https://doi.org/10.5194/acp-8-4141-2008, 2008.

Bash, J. O., Baker, K. R., and Beaver, M. R.: Evaluation of improved land use and canopy representation in BEIS v3.61 with biogenic VOC measurements in California, Geoscientific Model Development, 9, 2191–2207, https://doi.org/10.5194/gmd-9-2191-2016, 2016.

Bloss, C., Wagner, V., Jenkin, M. E., Volkamer, R., Bloss, W. J., Lee, J. D., Heard, D. E., Wirtz, K., Martin-Reviejo, M., Rea, G., Wenger, J. C., and Pilling, M. J.: Development of a detailed chemical mechanism (MCMv3.1) for the atmospheric oxidation of aromatic hydrocarbons, Atmos. Chem. Phys., 5, 641–664, https://doi.org/10.5194/acp-5-641-2005, 2005.

Byun, D. and Schere, K. L.: Review of the Governing Equations, Computational Algorithms, and Other Components of the Models-3 Community Multiscale Air Quality (CMAQ) Modeling System, Applied Mechanics Reviews, 59, 51–77, https://doi.org/10.1115/1.2128636, 2006.

Cao, L., Sihler, H., Platt, U., and Gutheil, E.: Numerical analysis of the chemical kinetic mechanisms of ozone depletion and halogen release in the polar troposphere, Atmos. Chem. Phys., 14, 3771–3787, https://doi.org/10.5194/acp-14-3771-2014, 2014.

Cao, L., Wang, C., Mao, M., Grosshans, H., and Cao, N.: Derivation of the reduced reaction mechanisms of ozone depletion events in the Arctic spring by using concentration sensitivity analysis and principal component analysis, Atmos. Chem. Phys., 16, 14 853–14 873, https://doi.org/10.5194/acp-16-14853-2016, 2016.

Cao, L., Gao, M., Li, S., Yi, Z., and Meng, X.: Sensitivity analysis of the dependence of the Carbon Bond Mechanism IV (CBM-IV) on the initial air composition under an urban condition, Atmospheric Environment, 215, 116 860, https://doi.org/https://doi.org/10.1016/j.atmosenv.2019.116860, 2019.

Carter, W. P.: Documentation of the SAPRC-99 chemical mechanism for VOC reactivity assessment, Tech. Rep. 329, California Air Resources Board, 2000a.

Carter, W. P.: Implementation of the SAPRC-99 chemical mechanism into the Models-3 framework, Tech. rep., United States Environmental Protection Agency, 2000b.

https://doi.org/10.5194/acp-2020-1295
Preprint. Discussion started: 15 March 2021

Atmospheric Chemistry and Physics Discussions

Carter, W. P.: Development of the SAPRC-07 chemical mechanism, Atmos. Environ., 44, 5324 – 5335, https://doi.org/https://doi.org/10.1016/j.atmosenv.2010.01.026, 2010.

Crowley, J. N., Ammann, M., Cox, R. A., Hynes, R. G., Jenkin, M. E., Mellouki, A., Rossi, M. J., Troe, J., and Wallington, T. J.: Evaluated kinetic and photochemical data for atmospheric chemistry: Volume V – heterogeneous reactions on solid substrates, Atmospheric Chemistry and Physics, 10, 9059–9223, https://doi.org/10.5194/acp-10-9059-2010, 2010.

Emery, C., Jung, J., Koo, B., and Yarwood, G.: Final Reprot, Improvements to CAMx Snow Cover Treatments and Carbon Bond Chemical Mechanism for Winter Ozone, Tech. rep., Ramboll Environ, 2015.

Emery, C., Koo, B., Hsieh, W., Wentland, A., Wilson, G., and Yarwood, G.: Technical Memorandum to Chris Misenis at U.S. EPA, Tech. rep., 2016.

Emmons, L. K., Walters, S., Hess, P. G., Lamarque, J.-F., Pfister, G. G., Fillmore, D., Granier, C., Guenther, A., Kinnison, D., Laepple, T., Orlando, J., Tie, X., Tyndall, G., Wiedinmyer, C., Baughcum, S. L., and Kloster, S.: Description and evaluation of the Model for Ozone and Related chemical Tracers, version 4 (MOZART-4), Geoscientific Model Development, 3, 43–67, https://doi.org/10.5194/gmd-3-43-2010, https://gmd.copernicus.org/articles/3/43/2010/, 2010.

ENVIRON: User's Guide: Comprehensive Air Quality Model with Extensions (CAMx), Version 6.50, Tech. rep., 2015.

Gery, M. W., Whitten, G. Z., Killus, J. P., and Dodge, M. C.: A photochemical kinetics mechanism for urban and regional scale computer modeling, J. Geophys. Res. Atmos., 94, 12 925–12 956, 1989.

Grell, G. A., Peckham, S. E., Schmitz, R., McKeen, S. A., Frost, G., Skamarock, W. C., and Eder, B.: Fully coupled "online" chemistry within the WRF model, Atmos. Environ., 39, 6957 – 6975, https://doi.org/https://doi.org/10.1016/j.atmosenv.2005.04.027, 2005.

Guenther, A., Karl, T., Harley, P., Wiedinmyer, C., Palmer, P. I., and Geron, C.: Estimates of global terrestrial isoprene emissions using MEGAN (Model of Emissions of Gases and Aerosols from Nature), Atmospheric Chemistry and Physics, 6, 3181–3210, https://doi.org/10.5194/acp-6-3181-2006, 2006.

Guenther, A. B., Jiang, X., Heald, C. L., Sakulyanontvittaya, T., Duhl, T., Emmons, L. K., and Wang, X.: The Model of Emissions of Gases and Aerosols from Nature version 2.1 (MEGAN2.1): an extended and updated framework for modeling biogenic emissions, Geoscientific Model Development, 5, 1471–1492, https://doi.org/10.5194/gmd-5-1471-2012, 2012.

Jenkin, M. E., Saunders, S. M., and Pilling, M. J.: The tropospheric degradation of volatile organic compounds: a protocol for mechanism development, Atmos. Environ., 31, 81–104, https://doi.org/https://doi.org/10.1016/S1352-2310(96)00105-7, 1997.

Jenkin, M. E., Saunders, S. M., Wagner, V., and Pilling, M. J.: Protocol for the development of the Master Chemical Mechanism, MCM v3 (Part B): tropospheric degradation of aromatic volatile organic compounds, Atmos. Chem. Phys., 3, 181–193, https://doi.org/10.5194/acp-3-181-2003, 2003.

Jenkin, M. E., Wyche, K. P., Evans, C. J., Carr, T., Monks, P. S., Alfarra, M. R., Barley, M. H., McFiggans, G. B., Young, J. C., and Rickard, A. R.: Development and chamber evaluation of the MCM v3.2 degradation scheme for β-caryophyllene, Atmos. Chem. Phys., 12, 5275–5308, https://doi.org/10.5194/acp-12-5275-2012, 2012.

Jenkin, M. E., Young, J. C., and Rickard, A. R.: The MCM v3.3.1 degradation scheme for isoprene, Atmos. Chem. Phys., 15, 11 433–11 459, https://doi.org/10.5194/acp-15-11433-2015, 2015.

Luecken, D., Hutzell, W., and Gipson, G.: Development and analysis of air quality modeling simulations for hazardous air pollutants, Atmospheric Environment, 40, 5087 – 5096, https://doi.org/https://doi.org/10.1016/j.atmosenv.2005.12.044, 2006.

https://doi.org/10.5194/acp-2020-1295
Preprint. Discussion started: 15 March 2021

Atmospheric Chemistry and Physics Discussions

Luecken, D., Phillips, S., Sarwar, G., and Jang, C.: Effects of using the CB05 vs. SAPRC99 vs. CB4 chemical mechanism on model predictions: Ozone and gas-phase photochemical precursor concentrations, Atmospheric Environment, 42, 5805 – 5820, https://doi.org/https://doi.org/10.1016/j.atmosenv.2007.08.056, 2008.

Luecken, D., Yarwood, G., and Hutzell, W.: Multipollutant modeling of ozone, reactive nitrogen and HAPs across the continental US with CMAQ-CB6, Atmospheric Environment, 201, 62 – 72, https://doi.org/https://doi.org/10.1016/j.atmosenv.2018.11.060, 2019.

Luecken, D. J., Napelenok, S. L., Strum, M., Scheffe, R., and Phillips, S.: Sensitivity of Ambient Atmospheric Formaldehyde and Ozone to Precursor Species and Source Types Across the United States, Environmental Science & Technology, 52, 4668–4675, https://doi.org/10.1021/acs.est.7b05509, 2018.

Madronich, S. and Flocke, S.: Theoretical Estimation of Biologically Effective UV Radiation at the Earth's Surface, in: Solar Ultraviolet Radiation, edited by Zerefos, C. S. and Bais, A. F., pp. 23–48, Springer Berlin Heidelberg, Berlin, Heidelberg, 1997.

Madronich, S. and Flocke, S.: The Role of Solar Radiation in Atmospheric Chemistry, pp. 1–26, Springer Berlin Heidelberg, Berlin, Heidelberg, https://doi.org/10.1007/978-3-540-69044-3_1, 1999.

Marvin, M. R., Wolfe, G. M., Salawitch, R. J., Canty, T. P., Roberts, S. J., Travis, K. R., Aikin, K. C., de Gouw, J. A., Graus, M., Hanisco, T. F., Holloway, J. S., Hübler, G., Kaiser, J., Keutsch, F. N., Peischl, J., Pollack, I. B., Roberts, J. M., Ryerson, T. B., Veres, P. R., and Warneke, C.: Impact of evolving isoprene mechanisms on simulated formaldehyde: An inter-comparison supported by in situ observations from SENEX, Atmospheric Environment, 164, 325 – 336, https://doi.org/https://doi.org/10.1016/j.atmosenv.2017.05.049, 2017.

Pierce, T., Geron, C., Bender, L., Dennis, R., Tonnesen, G., and Guenther, A.: Influence of increased isoprene emissions on regional ozone modeling, Journal of Geophysical Research: Atmospheres, 103, 25 611–25 629, https://doi.org/https://doi.org/10.1029/98JD01804, 1998.

Ruiz Hildebrandt, L. and Yarwood, G.: Interactions between Organic Aerosol and NO_y: Influence on Oxidant Production, Tech. rep., 2013.

Sander, S. P., Finlayson-Pitts, B. J., Friedl, R. R., Golden, D. M., Huie, R. E., Keller-Rudek, H., Kolb, C. E., Kurylo, M. J., Molina, M. J., Moortgat, G. K., Orkin, V. L., Ravishankara, A. R., and Wine, P. W.: Chemical Kinetics and Photochemical Data for Use in Atmospheric Studies. Evaluation No. 15 (JPL Publication 06-2), Jet Propulsion Laboratory, Pasadena, CA, 2006.

Sandu, A., Verwer, J., Loon, M. V., Carmichael, G., and Seinfeld, J.: Benchmarking stiff ODE solvers for atmospheric chemistry problems I: implicit versus explicit, Atmos. Environ., 31, 3151–3166, 1997.

Saunders, S. M., Jenkin, M. E., Derwent, R. G., and Pilling, M. J.: Protocol for the development of the Master Chemical Mechanism, MCM v3 (Part A): tropospheric degradation of non-aromatic volatile organic compounds, Atmos. Chem. Phys., 3, 161–180, https://doi.org/10.5194/acp-3-161-2003, 2003.

Saylor, R. D. and Ford, G. D.: On the comparison of numerical methods for the integration of kinetic equations in atmospheric chemistry and transport models, Atmospheric Environment, 29, 2585 – 2593, https://doi.org/https://doi.org/10.1016/1352-2310(95)00187-4, 1995.

Stockwell, W. R., Saunders, E., Goliff, W. S., and Fitzgerald, R. M.: A Perspective on the Development of Gas-phase Chemical Mechanisms for Eulerian Air Quality Models, Journal of the Air & Waste Management Association (1995), 70, 2019.

Turányi, T.: KINAL - a program package for kinetic analysis of reaction mechanisms., Comput. Chem., 14, 253–254, 1990a.

Turányi, T.: Sensitivity analysis of complex kinetic systems. Tools and applications, J. Math. Chem., 5, 203–248, https://doi.org/10.1007/BF01166355, 1990b.

Whitten, G. Z., Heo, G., Kimura, Y., McDonald-Buller, E., Allen, D. T., Carter, W. P., and Yarwood, G.: A new condensed toluene mechanism for Carbon Bond: CB05-TU, Atmospheric Environment, 44, 5346 – 5355, https://doi.org/https://doi.org/10.1016/j.atmosenv.2009.12.029, 2010.

https://doi.org/10.5194/acp-2020-1295
Preprint. Discussion started: 15 March 2021

Atmospheric Chemistry and Physics Discussions

Wolfe, G. M., Kaiser, J., Hanisco, T. F., Keutsch, F. N., de Gouw, J. A., Gilman, J. B., Graus, M., Hatch, C. D., Holloway, J., Horowitz, L. W., Lee, B. H., Lerner, B. M., Lopez-Hilifiker, F., Mao, J., Marvin, M. R., Peischl, J., Pollack, I. B., Roberts, J. M., Ryerson, T. B., Thornton, J. A., Veres, P. R., and Warneke, C.: Formaldehyde production from isoprene oxidation across NO_x regimes, Atmospheric Chemistry and Physics, 16, 2597–2610, https://doi.org/10.5194/acp-16-2597-2016, 2016.

Yarwood, G., Rao, S., Yocke, M., and Whitten, G.: Updates to the carbon bond chemical mechanism: CB05, Tech. rep., U.S. Environmental Protection Agency, 2005.

Yarwood, G., Jung, J., Whitten, G., Heo, G., J, M., and M, E.: Updates to the Carbon Bond Mechanism for Version 6 (CB6), in: 9th Annual CMAS Conference, pp. 1–4, Chapel Hill, NC, 2010.

Yarwood, G., Heo, G., Carter, W., and GZ, W.: Final Report, Environmental Chamber Experiments to Evaluate NO_x Sinks and Recycling in Atmospheric Chemical Mechanisms, Tech. rep., Texas Air Quality Research Program, The University of Texas at Austin, 2012.

Zaveri, R. A. and Peters, L. K.: A new lumped structure photochemical mechanism for large-scale applications, J. Geophys. Res. Atmos., 104, 30 387–30 415, https://doi.org/10.1029/1999JD900876, 1999.

Zhang, Q., Jiang, X., Tong, D., Davis, S. J., Zhao, H., Geng, G., Feng, T., Zheng, B., Lu, Z., Streets, D. G., Ni, R., Brauer, M., van Donkelaar, A., Martin, R. V., Huo, H., Liu, Z., Pan, D., Kan, H., Yan, Y., Lin, J., He, K., and Guan, D.: Transboundary health impacts of transported global air pollution and international trade, Nature, 543, https://doi.org/10.1038/nature21712, 2017a.

Zhang, R., Cohan, A., Biazar, A. P., and Cohan, D. S.: Source apportionment of biogenic contributions to ozone formation over the United States, Atmospheric Environment, 164, 8–19, 2017b.

https://doi.org/10.5194/acp-2020-1295
Preprint. Discussion started: 15 March 2021

Atmospheric Chemistry and Physics Discussions

Table 1. The initial air composition and the surface emission intensity used in simulations. This initial condition was taken from Saylor and Ford (1995) and Sandu et al. (1997), and represents a heavily polluted environment with a 70% relative humidity.

Species	Initial Concentration (ppb)	Emission Intensity (ppb h^{-1})
NO	50	1.00
NO_2	20	0.20
HONO	1	-
O_3	100	-
CO	300	2.00
HCHO	10	0.20
ALD2	2.2	0.04
IOLE	6.7	0.13
ALDX	1.1	0.02
PAN	1	-
ETH	10	0.20
TOL	10	0.20
XYL	10	0.20
ISOP	10	1.00
PAR	50	2.00
OLE	10	1.00
H_2	560	-
CH_4	1850	-
H_2O	2.17×10^7	-

https://doi.org/10.5194/acp-2020-1295
Preprint. Discussion started: 15 March 2021

Atmospheric Chemistry and Physics Discussions

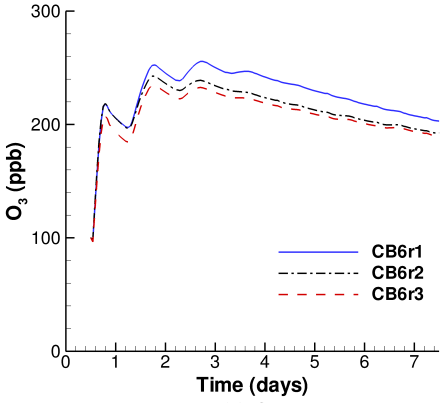

(a) O_3

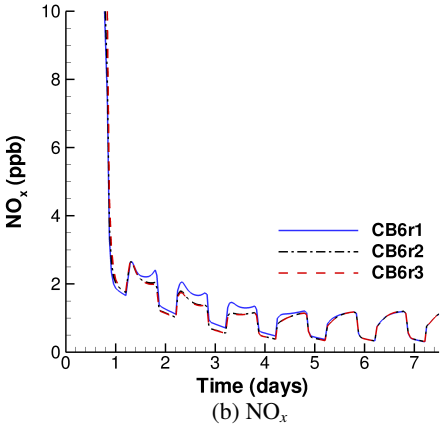

(b) NO_x

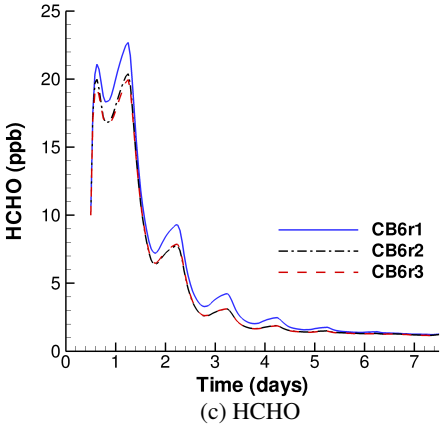

(c) HCHO

Figure 1. Simulated temporal evolutions of O_3, NO_x and HCHO by using different versions of the CB6 mechanism, when the surface emission is not included.

https://doi.org/10.5194/acp-2020-1295
Preprint. Discussion started: 15 March 2021

Atmospheric Chemistry and Physics Discussions

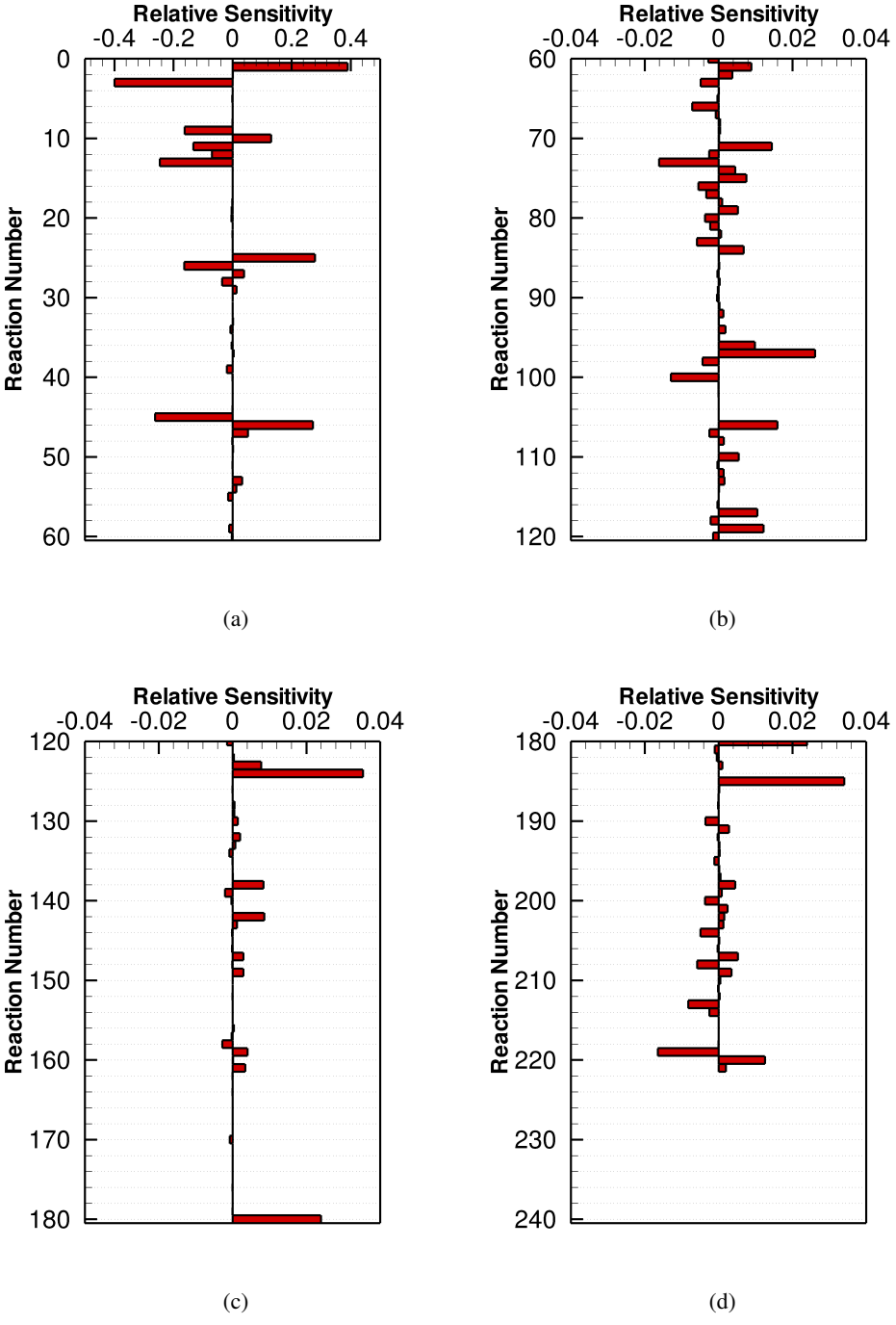

Figure 2. Averaged ozone sensitivity to the CB6r3 mechanism over the 7-th day, when the surface emission is excluded. Note that the horizontal scales of the sub-figures are different.

https://doi.org/10.5194/acp-2020-1295
Preprint. Discussion started: 15 March 2021

Atmospheric Chemistry and Physics Discussions

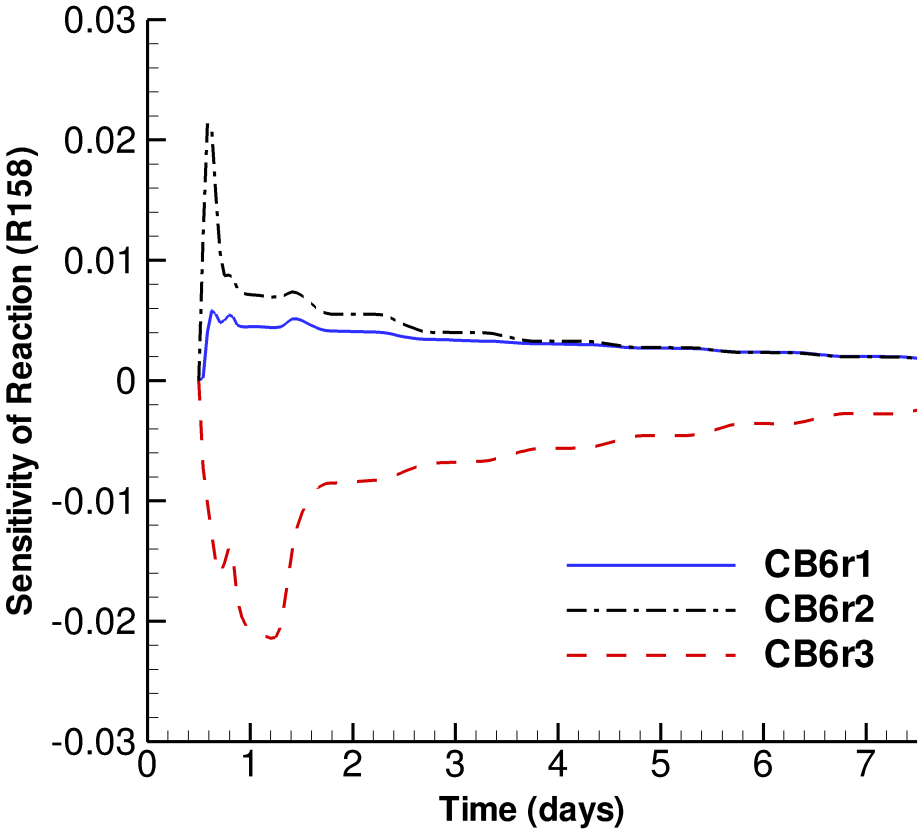

Figure 3. Temporal evolution of the ozone sensitivities to Reaction (R158) for different versions of the CB6 mechanism.

https://doi.org/10.5194/acp-2020-1295
Preprint. Discussion started: 15 March 2021

Atmospheric Chemistry and Physics Discussions

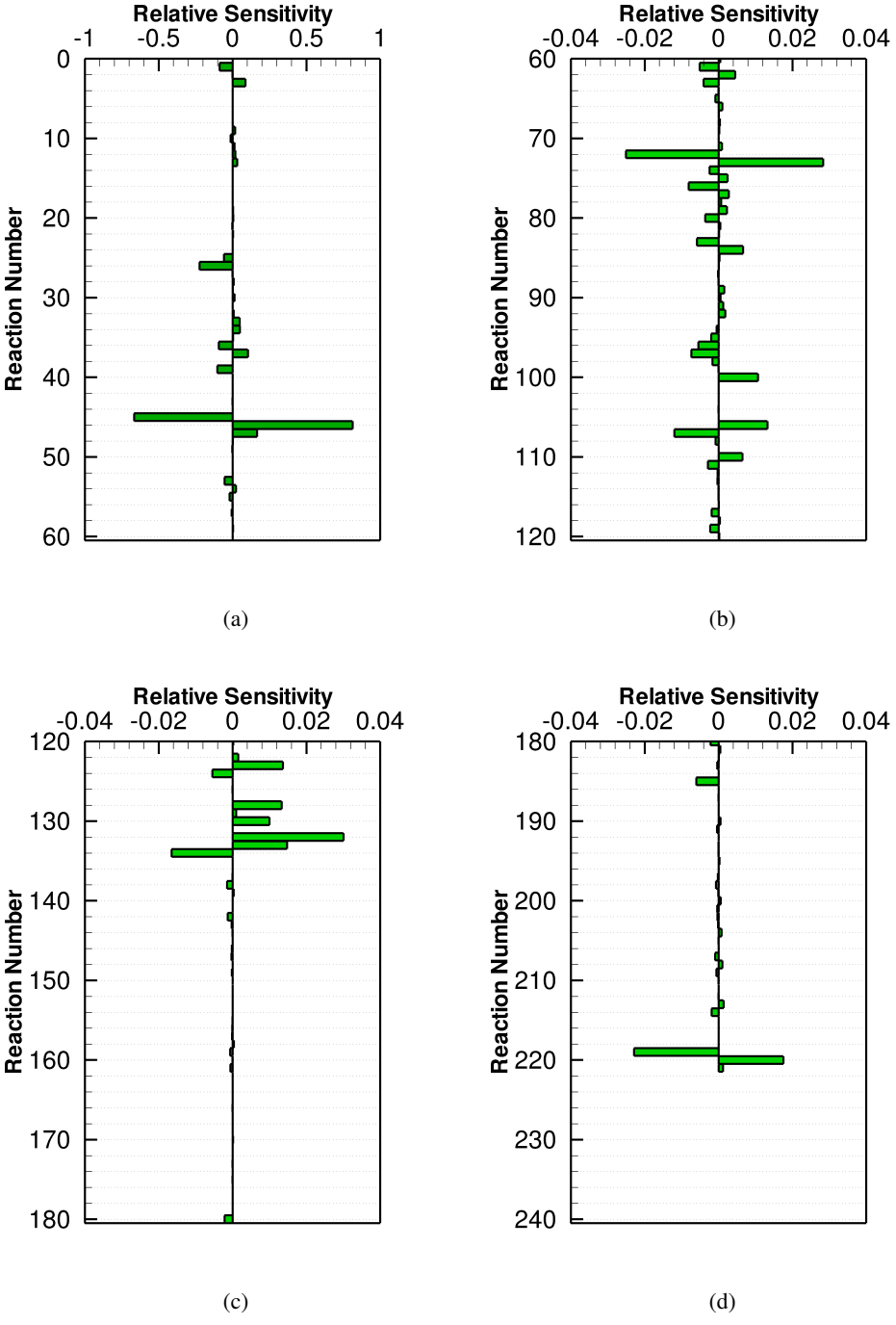

Figure 4. Averaged NO_x sensitivity to the CB6r3 mechanism over the 7-th day, when the surface emission is excluded. Note that the horizontal scales of the sub-figures are different.

https://doi.org/10.5194/acp-2020-1295
Preprint. Discussion started: 15 March 2021

Atmospheric Chemistry and Physics Discussions

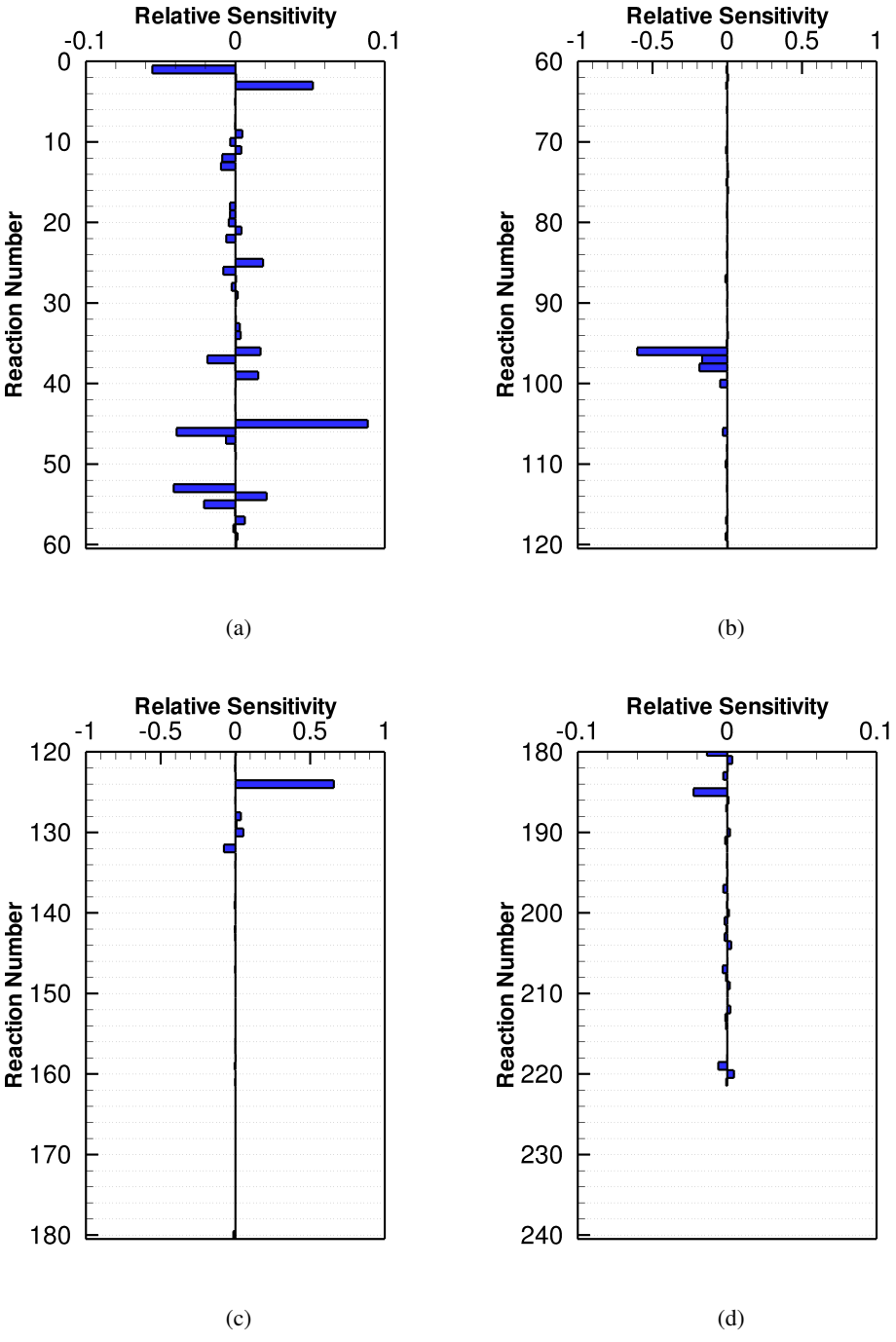

Figure 5. Averaged HCHO sensitivity to the CB6r3 mechanism over the 7-th day, when the surface emission is excluded. Note that the horizontal scales of the sub-figures are different.

https://doi.org/10.5194/acp-2020-1295
Preprint. Discussion started: 15 March 2021

Atmospheric Chemistry and Physics Discussions

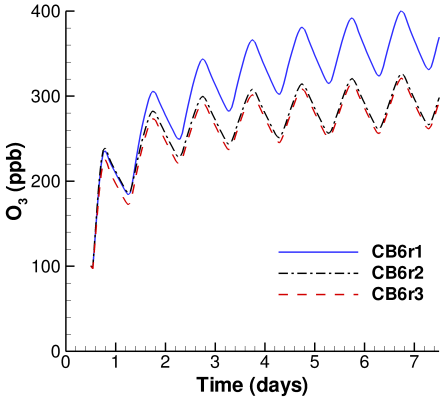

(a)

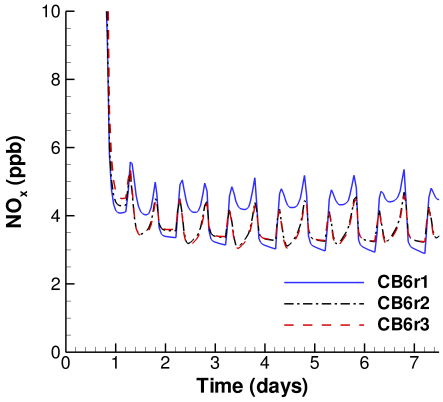

(b)

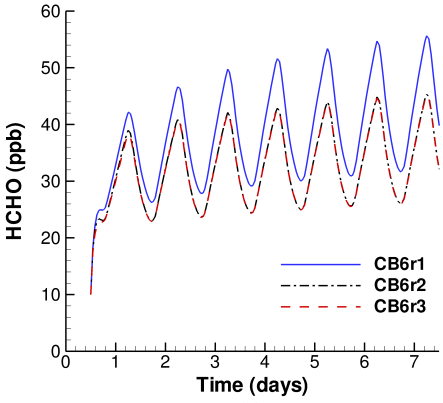

(c)

Figure 6. Simulated temporal evolution of O_3, NO_x and HCHO by using different versions of the CB6 mechanism, when the surface emission is included.

https://doi.org/10.5194/acp-2020-1295
Preprint. Discussion started: 15 March 2021

Atmospheric Chemistry and Physics Discussions

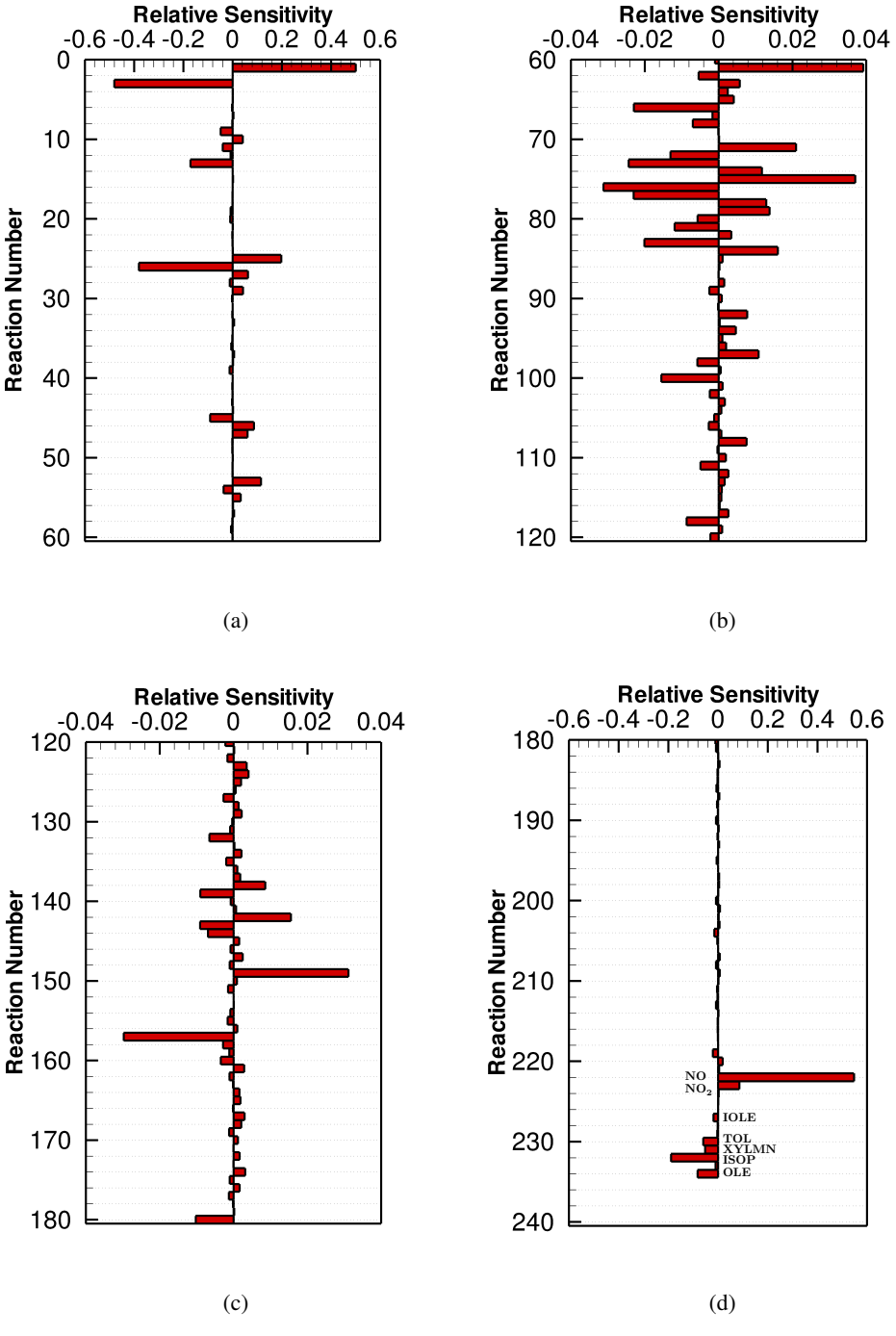

Figure 7. Averaged ozone sensitivity to the CB6r3 mechanism over the 7-th day, when the surface emission is included.

https://doi.org/10.5194/acp-2020-1295
Preprint. Discussion started: 15 March 2021

Atmospheric Chemistry and Physics Discussions

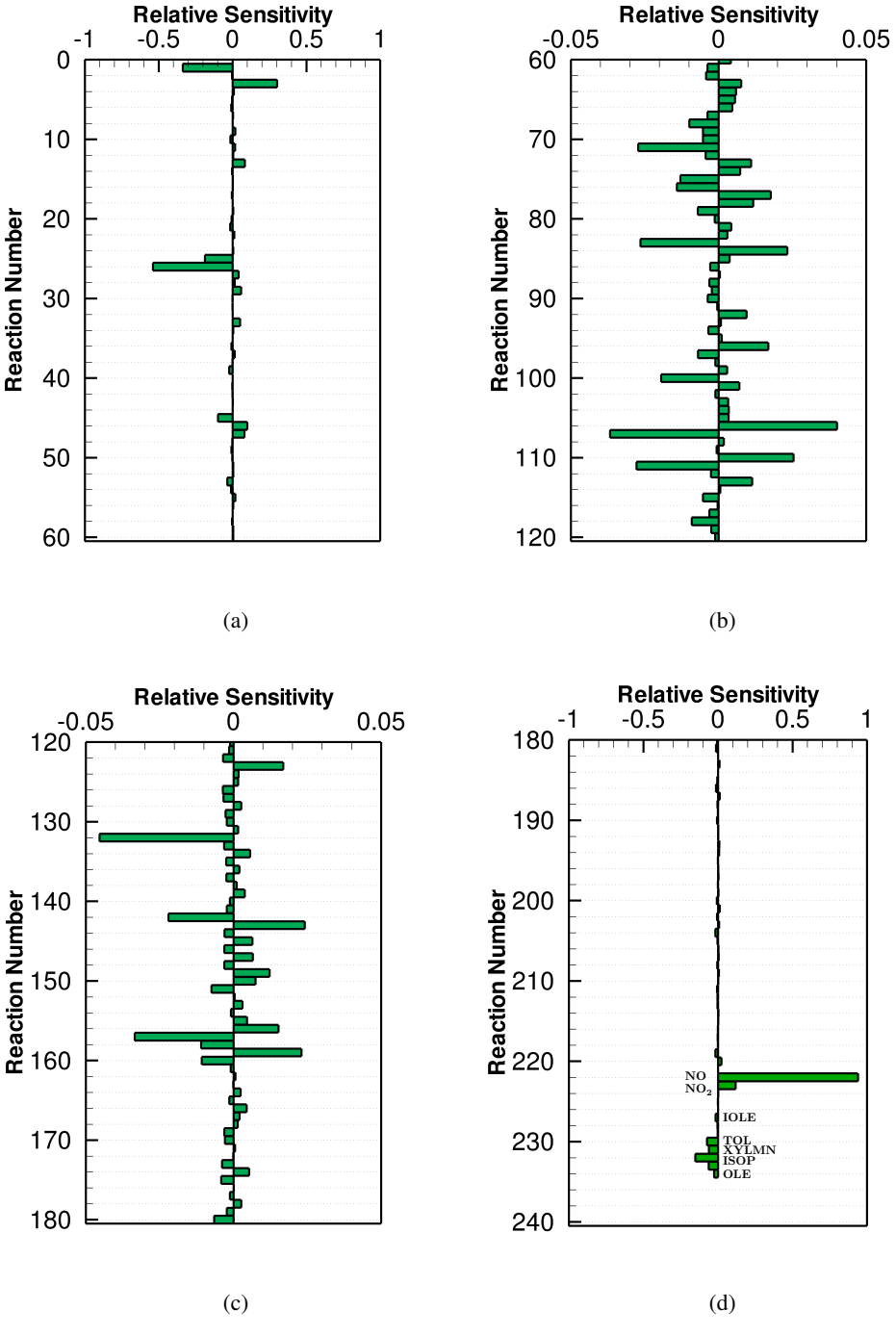

Figure 8. Averaged NO_x sensitivity to the CB6r3 mechanism over the 7-th day, when the surface emission is included.

https://doi.org/10.5194/acp-2020-1295
Preprint. Discussion started: 15 March 2021

Atmospheric Chemistry and Physics Discussions

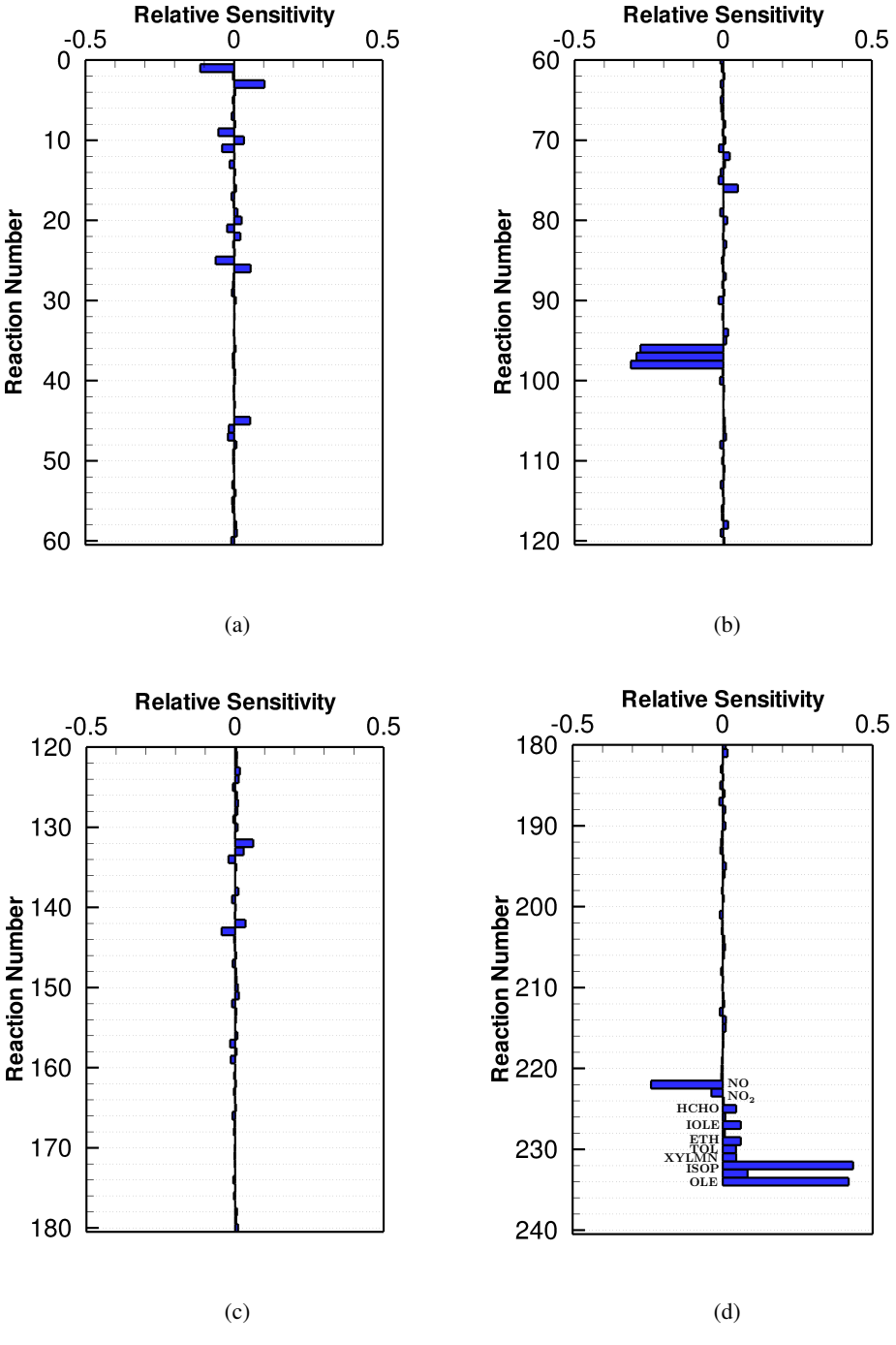

Figure 9. Averaged HCHO sensitivity to the CB6r3 mechanism over the 7-th day, when the surface emission is included.

https://doi.org/10.5194/acp-2020-1295
Preprint. Discussion started: 15 March 2021

Atmospheric Chemistry and Physics Discussions

Table A1. Complete listings of chemical reactions belonging to different CB6 mechanisms used in the present study. The updates between different versions of the CB6 mechanism are also marked. The abbreviation "-" denotes that there is no change in the form of this reaction between different CB6 mechanisms.

Reaction Number	CB6r1	Reaction Number	CB6r2	Reaction Number	CB6r3
(R1)	$NO_2 + h\nu \rightarrow NO + O$	(R1)	-	(R1)	-
(R2)	$O + O_2 + M \rightarrow O_3 + M$	(R2)	-	(R2)	-
(R3)	$O_3 + NO \rightarrow NO_2$	(R3)	-	(R3)	-
(R4)	$O + NO + M \rightarrow NO_2 + M$	(R4)	-	(R4)	-
(R5)	$O + NO_2 \rightarrow NO$	(R5)	-	(R5)	-
(R6)	$O + NO_2 \rightarrow NO_3$	(R6)	-	(R6)	-
(R7)	$O + O_3 \rightarrow$	(R7)	-	(R7)	-
(R8)	$O_3 + h\nu \rightarrow O$	(R8)	-	(R8)	-
(R9)	$O_3 + h\nu \rightarrow O(^1D)$	(R9)	-	(R9)	-
(R10)	$O(^1D) + M \rightarrow O + M$	(R10)	-	(R10)	-
(R11)	$O(^1D) + H_2O \rightarrow 2OH$	(R11)	-	(R11)	-
(R12)	$O_3 + OH \rightarrow HO_2$	(R12)	-	(R12)	-
(R13)	$O_3 + HO_2 \rightarrow OH$	(R13)	-	(R13)	-
(R14)	$OH + O \rightarrow HO_2$	(R14)	-	(R14)	-
(R15)	$HO_2 + O \rightarrow OH$	(R15)	-	(R15)	-
(R16)	$OH + OH \rightarrow O$	(R16)	-	(R16)	-
(R17)	$OH + OH \rightarrow H_2O_2$	(R17)	-	(R17)	-
(R18)	$OH + HO_2 \rightarrow$	(R18)	-	(R18)	-
(R19)	$HO_2 + HO_2 \rightarrow H_2O_2$	(R19)	-	(R19)	-
(R20)	$HO_2 + HO_2 + H_2O \rightarrow H_2O_2$	(R20)	-	(R20)	-
(R21)	$H_2O_2 + h\nu \rightarrow 2OH$	(R21)	-	(R21)	-
(R22)	$H_2O_2 + OH \rightarrow HO_2$	(R22)	-	(R22)	-
(R23)	$H_2O_2 + O \rightarrow OH + HO_2$	(R23)	-	(R23)	-
(R24)	$NO + NO + O_2 \rightarrow 2NO_2$	(R24)	-	(R24)	-
(R25)	$HO_2 + NO \rightarrow OH + NO_2$	(R25)	-	(R25)	-
(R26)	$NO_2 + O_3 \rightarrow NO_3$	(R26)	-	(R26)	-
(R27)	$NO_3 + h\nu \rightarrow NO_2 + O$	(R27)	-	(R27)	-
(R28)	$NO_3 + h\nu \rightarrow NO$	(R28)	-	(R28)	-
(R29)	$NO_3 + NO \rightarrow 2NO_2$	(R29)	-	(R29)	-
(R30)	$NO_3 + NO_2 \rightarrow NO + NO_2$	(R30)	-	(R30)	-

https://doi.org/10.5194/acp-2020-1295
Preprint. Discussion started: 15 March 2021

Atmospheric Chemistry and Physics Discussions

Table A1. (continued).

Reaction Number	CB6r1	Reaction Number	CB6r2	Reaction Number	CB6r3
(R31)	$NO_3 + O \rightarrow NO_2$	(R31)	-	(R31)	-
(R32)	$NO_3 + OH \rightarrow HO_2 + NO_2$	(R32)	-	(R32)	-
(R33)	$NO_3 + HO_2 \rightarrow OH + NO_2$	(R33)	-	(R33)	-
(R34)	$NO_3 + O_3 \rightarrow NO_2$	(R34)	-	(R34)	-
(R35)	$NO_3 + NO_3 \rightarrow 2NO_2$	(R35)	-	(R35)	-
(R36)	$NO_3 + NO_2 \rightarrow N_2O_5$	(R36)	-	(R36)	-
(R37)	$N_2O_5 \rightarrow NO_3 + NO_2$	(R37)	-	(R37)	-
(R38)	$N_2O_5 + h\nu \rightarrow NO_3 + NO_2$	(R38)	-	(R38)	-
(R39)	$N_2O_5 + H_2O \rightarrow 2HNO_3$	(R39)	-	(R39)	-
(R40)	$NO + OH \rightarrow HONO$	(R40)	-	(R40)	-
(R41)	$NO + NO_2 + H_2O \rightarrow 2HONO$	(R41)	-	(R41)	-
(R42)	$HONO + HONO \rightarrow NO + NO_2$	(R42)	-	(R42)	-
(R43)	$HONO + h\nu \rightarrow NO + OH$	(R43)	-	(R43)	-
(R44)	$HONO + OH \rightarrow NO_2$	(R44)	-	(R44)	-
(R45)	$NO_2 + OH \rightarrow HNO_3$	(R45)	-	(R45)	-
(R46)	$HNO_3 + OH \rightarrow NO_3$	(R46)	-	(R46)	-
(R47)	$HNO_3 + h\nu \rightarrow OH + NO_2$	(R47)	-	(R47)	-
(R48)	$HO_2 + NO_2 \rightarrow PNA$	(R48)	-	(R48)	-
(R49)	$PNA \rightarrow HO_2 + NO_2$	(R49)	-	(R49)	-
(R50)	$PNA + h\nu \rightarrow 0.59HO_2 + 0.59NO_2 + 0.41OH + 0.41NO_3$	(R50)	-	(R50)	-
(R51)	$PNA + OH \rightarrow NO_2$	(R51)	-	(R51)	-
(R52)	$SO2 + OH \rightarrow SULF + HO_2$	(R52)	-	(R52)	-
(R53)	$C2O3 + NO \rightarrow NO_2 + MEO2 + RO2$	(R53)	-	(R53)	-
(R54)	$C2O3 + NO_2 \rightarrow PAN$	(R54)	-	(R54)	-
(R55)	$PAN \rightarrow C2O3 + NO_2$	(R55)	-	(R55)	-
(R56)	$PAN + h\nu \rightarrow 0.6NO_2 + 0.6C2O3 + 0.4NO_3 + 0.4MEO2 + 0.4RO2$	(R56)	-	(R56)	-
(R57)	$C2O3 + HO_2 \rightarrow 0.41PACD + 0.15AACD + 0.15O_3 + 0.44MEO2 + 0.44RO2 + 0.44OH$	(R57)	-	(R57)	-
(R58)	$C2O3 + RO2 \rightarrow C2O3$	(R58)	-	(R58)	-
(R59)	$C2O3 + C2O3 \rightarrow 2MEO2 + 2RO2$	(R59)	-	(R59)	-
(R60)	$C2O3 + CXO3 \rightarrow MEO2 + ALD2 + XO2H + 2RO2$	(R60)	-	(R60)	-

https://doi.org/10.5194/acp-2020-1295
Preprint. Discussion started: 15 March 2021

Atmospheric Chemistry and Physics Discussions

Table A1. (continued).

Reaction Number	CB6r1	Reaction Number	CB6r2	Reaction Number	CB6r3
(R61)	$CXO3 + NO \rightarrow NO_2 + ALD2 + XO2H + RO2$	(R61)	-	(R61)	-
(R62)	$CXO3 + NO_2 \rightarrow PANX$	(R62)	-	(R62)	-
(R63)	$PANX \rightarrow NO_2 + CXO3$	(R63)	-	(R63)	-
(R64)	$PANX + h\nu \rightarrow 0.6NO_2 + 0.6CXO3 + 0.4NO_3 + 0.4ALD2 + 0.4XO2H + 0.4RO2$	(R64)	-	(R64)	-
(R65)	$CXO3 + HO_2 \rightarrow 0.41PACD + 0.15AACD + 0.15O_3 + 0.44ALD2 + 0.44XO2H + 0.44RO2 + 0.44OH$	(R65)	-	(R65)	-
(R66)	$CXO3 + RO2 \rightarrow CXO3$	(R66)	$CXO3 + RO2 \rightarrow 0.8ALD2 + 0.8XO2H + 0.8RO2$	(R66)	-
(R67)	$CXO3 + CXO3 \rightarrow 2ALD2 + 2XO2H + 2RO2$	(R67)	-	(R67)	-
(R68)	$RO2 + NO \rightarrow NO$	(R68)	-	(R68)	-
(R69)	$RO2 + HO_2 \rightarrow HO_2$	(R69)	-	(R69)	-
(R70)	$RO2 + RO2 \rightarrow$	(R70)	-	(R70)	-
(R71)	$MEO2 + NO \rightarrow HCHO + HO_2 + NO_2$	(R71)	-	(R71)	-
(R72)	$MEO2 + HO_2 \rightarrow 0.9MEPX + 0.1HCHO$	(R72)	-	(R72)	-
(R73)	$MEO2 + C2O3 \rightarrow HCHO + 0.9HO_2 + 0.9MEO2 + 0.1AACD + 0.9RO2$	(R73)	-	(R73)	-
(R74)	$MEO2 + RO2 \rightarrow 0.685HCHO + 0.315MEOH + 0.37HO_2 + RO2$	(R74)	-	(R74)	-
(R75)	$XO2H + NO \rightarrow NO_2 + HO_2$	(R75)	-	(R75)	-
(R76)	$XO2H + HO_2 \rightarrow ROOH$	(R76)	-	(R76)	-
(R77)	$XO2H + C2O3 \rightarrow 0.8HO_2 + 0.8MEO2 + 0.2AACD + 0.8RO2$	(R77)	-	(R77)	-
(R78)	$XO2H + RO2 \rightarrow 0.6HO_2 + RO2$	(R78)	-	(R78)	-
(R79)	$XO2 + NO \rightarrow NO_2$	(R79)	-	(R79)	-
(R80)	$XO2 + HO_2 \rightarrow ROOH$	(R80)	-	(R80)	-
(R81)	$XO2 + C2O3 \rightarrow 0.8MEO2 + 0.2AACD + 0.8RO2$	(R81)	-	(R81)	-
(R82)	$XO2 + RO2 \rightarrow 0.6HO_2 + RO2$	(R82)	$XO2 + RO2 \rightarrow RO2$	(R82)	-
(R83)	$XO2N + NO \rightarrow NTR$	(R83)	$XO2N + NO \rightarrow 0.5NTR1 + 0.5NTR2$	(R83)	-
(R84)	$XO2N + HO_2 \rightarrow ROOH$	(R84)	-	(R84)	-
(R85)	$XO2N + C2O3 \rightarrow 0.8HO_2 + 0.8MEO2 + 0.2AACD + 0.8RO2$	(R85)	-	(R85)	-

https://doi.org/10.5194/acp-2020-1295
Preprint. Discussion started: 15 March 2021

Atmospheric Chemistry and Physics Discussions

Table A1. (continued).

Reaction Number	CB6r1	Reaction Number	CB6r2	Reaction Number	CB6r3
(R86)	$XO2N + RO2 \rightarrow 0.6HO_2 + RO2$	(R86)	$XO2N + RO2 \rightarrow RO2$	(R86)	-
(R87)	$MEPX + OH \rightarrow 0.6MEO2 + 0.6RO2 + 0.4HCHO + 0.4OH$	(R87)	-	(R87)	-
(R88)	$MEPX + h\nu \rightarrow MEO2 + RO2 + OH$	(R88)	-	(R88)	-
(R89)	$ROOH + OH \rightarrow 0.54XO2H + 0.06XO2N + 0.6RO2 + 0.4OH$	(R89)	-	(R89)	-
(R90)	$ROOH + h\nu \rightarrow HO_2 + OH$	(R90)	-	(R90)	-
(R91)	$NTR + OH \rightarrow HNO_3 + XO2H + RO2$	(R91)	$NTR1 + OH \rightarrow NTR2$	(R91)	-
(R92)	$NTR + h\nu \rightarrow NO_2 + XO2H + RO2$	(R92)	$NTR1 + h\nu \rightarrow NO_2$	(R92)	-
(R93)	$FACD + OH \rightarrow HO_2$	(R93)	-	(R93)	-
(R94)	$AACD + OH \rightarrow MEO2 + RO2$	(R94)	-	(R94)	-
(R95)	$PACD + OH \rightarrow C2O3$	(R95)	-	(R95)	-
(R96)	$HCHO + OH \rightarrow HO_2 + CO$	(R96)	-	(R96)	-
(R97)	$HCHO + h\nu \rightarrow 2HO_2 + CO$	(R97)	-	(R97)	-
(R98)	$HCHO + h\nu \rightarrow CO$	(R98)	-	(R98)	-
(R99)	$HCHO + O \rightarrow OH + HO_2 + CO$	(R99)	-	(R99)	-
(R100)	$HCHO + NO_3 \rightarrow HNO_3 + HO_2 + CO$	(R100)	-	(R100)	-
(R101)	$HCHO + HO_2 \rightarrow HCO3$	(R101)	-	(R101)	-
(R102)	$HCO3 \rightarrow HCHO + HO_2$	(R102)	-	(R102)	-
(R103)	$HCO3 + NO \rightarrow FACD + NO_2 + HO_2$	(R103)	-	(R103)	-
(R104)	$HCO3 + HO_2 \rightarrow 0.5MEPX + 0.5FACD + 0.2OH + 0.2HO_2$	(R104)	-	(R104)	-
(R105)	$ALD2 + O \rightarrow C2O3 + OH$	(R105)	-	(R105)	-
(R106)	$ALD2 + OH \rightarrow C2O3$	(R106)	-	(R106)	-
(R107)	$ALD2 + NO_3 \rightarrow C2O3 + HNO_3$	(R107)	-	(R107)	-
(R108)	$ALD2 + h\nu \rightarrow MEO2 + RO2 + CO + HO_2$	(R108)	-	(R108)	-
(R109)	$ALDX + O \rightarrow CXO3 + OH$	(R109)	-	(R109)	-
(R110)	$ALDX + OH \rightarrow CXO3$	(R110)	-	(R110)	-
(R111)	$ALDX + NO_3 \rightarrow CXO3 + HNO_3$	(R111)	-	(R111)	-
(R112)	$ALDX + h\nu \rightarrow MEO2 + RO2 + CO + HO_2$	(R112)	$ALDX + h\nu \rightarrow ALD2 + XO2H + RO2 + CO + HO_2$	(R112)	-
(R113)	$GLYD + OH \rightarrow 0.2GLY + 0.2HO_2 + 0.8C2O3$	(R113)	-	(R113)	-

https://doi.org/10.5194/acp-2020-1295
Preprint. Discussion started: 15 March 2021

Atmospheric Chemistry and Physics Discussions

Table A1. (continued).

Reaction Number	CB6r1	Reaction Number	CB6r2	Reaction Number	CB6r3
(R114)	$GLYD + h\nu \rightarrow 0.74HCHO + 0.89CO + 1.4HO_2 + 0.15MEOH + 0.19OH + 0.11GLY + 0.11XO2H + 0.11RO2$	(R114)	-	(R114)	-
(R115)	$GLYD + NO_3 \rightarrow HNO_3 + C2O3$	(R115)	-	(R115)	-
(R116)	$GLY + OH \rightarrow 1.7CO + 0.3XO2 + 0.3RO2 + HO_2$	(R116)	$GLY + OH \rightarrow 1.8CO + 0.2XO2 + 0.2RO2 + HO_2$	(R116)	-
(R117)	$GLY + h\nu \rightarrow 2HO_2 + 2CO$	(R117)	-	(R117)	-
(R118)	$GLY + NO_3 \rightarrow HNO_3 + CO + HO_2 + XO2 + RO2$	(R118)	$GLY + NO_3 \rightarrow HNO_3 + 1.5CO + 0.5XO2 + 0.5RO2 + HO_2$	(R118)	-
(R119)	$MGLY + h\nu \rightarrow C2O3 + HO_2 + CO$	(R119)	-	(R119)	-
(R120)	$MGLY + NO_3 \rightarrow HNO_3 + C2O3 + XO2 + RO2$	(R120)	-	(R120)	-
(R121)	$MGLY + OH \rightarrow C2O3 + CO$	(R121)	-	(R121)	-
(R122)	$H_2 + OH \rightarrow HO_2$	(R122)	-	(R122)	-
(R123)	$CO + OH \rightarrow HO_2$	(R123)	-	(R123)	-
(R124)	$CH_4 + OH \rightarrow MEO2 + RO_2$	(R124)	-	(R124)	-
(R125)	$ETHA + OH \rightarrow 0.991ALD2 + 0.991XO2H + 0.009XO2N + RO_2$	(R125)	-	(R125)	-
(R126)	$MEOH + OH \rightarrow HCHO + HO_2$	(R126)	-	(R126)	-
(R127)	$ETOH + OH \rightarrow 0.95ALD2 + 0.9HO_2 + 0.1XO2H + 0.1RO_2 + 0.078HCHO + 0.011GLYD$	(R127)	-	(R127)	-
(R128)	$KET + h\nu \rightarrow 0.5ALD2 + 0.5C2O3 + 0.5XO2H + 0.5CXO3 + 0.5MEO2 + RO2 - 2.5PAR$	(R128)	-	(R128)	-
(R129)	$ACET + h\nu \rightarrow 0.38CO + 1.38MEO2 + 1.38RO2 + 0.62C2O3$	(R129)	-	(R129)	-
(R130)	$ACET + OH \rightarrow HCHO + C2O3 + XO2 + RO2$	(R130)	-	(R130)	-
(R131)	$PRPA + OH \rightarrow 0.71ACET + 0.26ALDX + 0.26PAR + 0.97XO2H + 1.00RO2 + 0.03XO2N$	(R131)	-	(R131)	$PRPA + OH \rightarrow XPRP$
(R132)	$PAR + OH \rightarrow 0.11ALDX + 0.76ROR + 0.11XO2H + 0.76XO2 + RO2 - 0.11PAR + 0.13XO2N$	(R132)	-	(R132)	$PAR + OH \rightarrow XPAR$ -
(R133)	$ROR \rightarrow 0.2KET + 0.42ACET + 0.74ALD2 + 0.37ALDX + 0.04XO2N + 0.94XO2H + 0.98RO2 + 0.02ROR - 2.7PAR$	(R133)	-	(R133)	-
(R134)	$ROR + O_2 \rightarrow KET + HO_2$	(R134)	-	(R134)	-
(R135)	$ROR + NO_2 \rightarrow NTR$	(R135)	$ROR + NO_2 \rightarrow NTR2$	(R135)	$ROR + NO_2 \rightarrow NTR1$
(R136)	$ETHY + OH \rightarrow 0.7GLY + 0.7OH + 0.3FACD + 0.3CO + 0.3HO_2$	(R136)	-	(R136)	-
(R137)	$ETH + O \rightarrow HCHO + HO_2 + CO + 0.7XO2H + 0.7RO2 + 0.3OH$	(R137)	-	(R137)	-

https://doi.org/10.5194/acp-2020-1295
Preprint. Discussion started: 15 March 2021

Atmospheric Chemistry and Physics Discussions

Table A1. (continued).

Reaction Number	CB6r1	Reaction Number	CB6r2	Reaction Number	CB6r3
(R138)	$ETH + OH \rightarrow XO2H + RO2 + 1.56HCHO + 0.22GLYD$	(R138)	-	(R138)	-
(R139)	$ETH + O_3 \rightarrow HCHO + 0.51CO + 0.16HO_2 + 0.16OH + 0.37FACD$	(R139)	-	(R139)	-
(R140)	$ETH + NO_3 \rightarrow 0.5NO_2 + 0.5NTR + 0.5XO2H + 0.5XO2 + RO2 + 1.12HCHO$	(R140)	$ETH + NO_3 \rightarrow 0.5NO_2 + 0.5NTR1 + 0.5XO2H + 0.5XO2 + RO2 + 1.12HCHO$	(R140)	-
(R141)	$OLE + O \rightarrow 0.2ALD2 + 0.3ALDX + 0.1HO_2 + 0.2XO2H + 0.2CO + 0.2HCHO + 0.01XO2N + 0.21RO2 + 0.2PAR + 0.1OH$	(R141)	-	(R141)	-
(R142)	$OLE + OH \rightarrow 0.78HCHO + 0.49ALD2 + 0.49ALDX + 0.98XO2H + 0.2XO2 + 0.02XO2N + 1.2RO2 - 0.73PAR$	(R142)	-	(R142)	-
(R143)	$OLE + O_3 \rightarrow 0.29ALD2 + 0.56HCHO + 0.27ALDX + 0.15XO2H + 0.15RO2 + 0.33OH + 0.08HO_2 + 0.38CO + 0.07GLY + 0.07MGLY + 0.09FACD + 0.13AACD + 0.04H_2O_2 - 0.79PAR$	(R143)	-	(R143)	-
(R144)	$OLE + NO_3 \rightarrow 0.5NO_2 + 0.5NTR + 0.48XO2 + 0.48XO2H + 0.04XO2N + RO2 + 0.5HCHO + 0.25ALD2 + 0.38ALDX - PAR$	(R144)	$OLE + NO_3 \rightarrow 0.5NO_2 + 0.5NTR1 + 0.48XO2 + 0.48XO2H + 0.04XO2N + RO2 + 0.5HCHO + 0.25ALD2 + 0.38ALDX - PAR$	(R144)	-
(R145)	$IOLE + O \rightarrow 1.24ALD2 + 0.66ALDX + 0.1XO2H + 0.1RO2 + 0.1CO + 0.1PAR$	(R145)	-	(R145)	-
(R146)	$IOLE + OH \rightarrow 1.30ALD2 + 0.7ALDX + XO2H + RO2$	(R146)	-	(R146)	-
(R147)	$IOLE + O_3 \rightarrow 0.73ALD2 + 0.44ALDX + 0.13HCHO + 0.24CO + 0.5OH + 0.3XO2H + 0.3RO2 + 0.24GLY + 0.06MGLY + 0.29PAR + 0.08AACD + 0.08H_2O_2$	(R147)	-	(R147)	-
(R148)	$IOLE + NO_3 \rightarrow 0.5NO_2 + 0.5NTR + 0.48XO2 + 0.48XO2H + 0.04XO2N + RO2 + 0.5ALD2 + 0.62ALDX + PAR$	(R148)	$IOLE + NO_3 \rightarrow 0.5NO_2 + 0.5NTR1 + 0.48XO2 + 0.48XO2H + 0.04XO2N + RO2 + 0.5ALD2 + 0.62ALDX + PAR$	(R148)	-
(R149)	$ISOP + OH \rightarrow ISO2 + RO2 + ISOPRXN$	(R149)	-	(R149)	-
(R150)		(R150)	$ISOP + O \rightarrow 0.75ISPD + 0.5HCHO + 0.25XO2 + 0.25RO2 + 0.25HO_2 + 0.25CXO3 + 0.25PAR$	(R150)	-
(R151)	$ISO2 + NO \rightarrow 0.12INTR + 0.88NO_2 + 0.8HO_2 + 0.66HCHO + 0.66ISPD + 0.08XO2H + 0.08RO2 + 0.05IOLE + 0.04GLYD + 0.12PAR + 0.04GLY + 0.04MGLY + 0.09OLE + 0.12ALDX$	(R151)	$ISO2 + NO \rightarrow 0.1INTR + 0.9NO_2 + 0.67HCHO + 0.9ISPD + 0.82HO_2 + 0.08XO2H + 0.08RO2$	(R151)	-

https://doi.org/10.5194/acp-2020-1295
Preprint. Discussion started: 15 March 2021

Atmospheric Chemistry and Physics Discussions

Table A1. (continued).

Reaction Number	CB6r1	Reaction Number	CB6r2	Reaction Number	CB6r3
(R152)	$ISO2 + HO_2 \rightarrow 0.88ISPX + 0.12OH + 0.12HO_2 + 0.12HCHO + 0.12ISPD$	(R152)	-	(R152)	-
(R153)	$ISO2 + C2O3 \rightarrow 0.71HO_2 + 0.58HCHO + 0.58ISPD + 0.07XO2H + 0.04IOLE + 0.04GLYD + 0.1PAR + 0.03GLY + 0.04MGLY + 0.08OLE + 0.1ALDX + 0.8MEO2 + 0.2AACD + 0.87RO2$	(R153)	$ISO2 + C2O3 \rightarrow 0.6HCHO + ISPD + 0.73HO_2 + 0.07XO2H + 0.8MEO2 + 0.2AACD + 0.87RO2$	(R153)	-
(R154)	$ISO2 + RO2 \rightarrow 0.8HO_2 + 0.66HCHO + 0.66ISPD + 0.08XO2H + 0.05IOLE + 0.04GLYD + 0.12PAR + 0.04GLY + 0.04MGLY + 0.09OLE + 0.12ALDX + 1.08RO2$	(R154)	$ISO2 + RO2 \rightarrow 0.6HCHO + ISPD + 0.73HO_2 + 0.07XO2H + 1.07RO2$	(R154)	-
(R155)	$ISO2 \rightarrow 0.8HO_2 + 0.04OH + 0.04HCHO + 0.8ISPD$	(R155)	$ISO2 \rightarrow HO_2 + HPLD$	(R155)	-
(R156)	$ISOP + O_3 \rightarrow 0.6HCHO + 0.65ISPD + 0.15ALDX + 0.2CXO3 + 0.35PAR + 0.27OH + 0.2XO2 + 0.2RO2 + 0.07HO_2 + 0.07CO$	(R156)	-	(R156)	-
(R157)	$ISOP + NO_3 \rightarrow 0.35NO_2 + 0.65INTR + 0.64XO2H + 0.33XO2 + 0.03XO2N + RO2 + 0.35HCHO + 0.35ISPD + ISOPRXN$	(R157)	$ISOP + NO_3 \rightarrow 0.35NO_2 + 0.65NTR2 + 0.64XO2H + 0.33XO2 + 0.03XO2N + RO2 + 0.35HCHO + 0.35ISPD + ISOPRXN$	(R157)	-
(R158)	$ISPD + OH \rightarrow 0.1XO2N + 0.38XO2 + 0.32XO2H + 0.79RO2 + 0.84PAR + 0.38C2O3 + 0.21CXO3 + 0.38GLYD + 0.24MGLY + 0.24HCHO + 0.07OLE + 0.08CO + 0.03ALDX$	(R158)	$ISPD + OH \rightarrow 0.06XO2N + 0.52XO2 + 0.24XO2H + 0.15MGLY + 0.27MEO2 + 0.12GLY + 0.35GLYD + 0.23C2O3 + 0.12CXO3 + 0.24PAR + 0.26ACET + 0.2CO + 0.14HO_2 + 1.09RO2$	(R158)	$ISPD + OH \rightarrow 0.02XO2N + 0.52XO2 + 0.12MGLY + 0.12MEO2 + 0.27GLYD + 0.27C2O3 + 0.46OPO3 + 0.12PAR + 0.14ACET + 0.14CO + 0.14HO_2 + 0.66RO2$
(R159)	$ISPD + O_3 \rightarrow 0.02ALD2 + 0.15HCHO + 0.23CO + 0.85MGLY + 0.36PAR + 0.11C2O3 + 0.06XO2H + 0.06RO2 + 0.27OH + 0.09HO_2$	(R159)	$ISPD + O_3 \rightarrow 0.04ALD2 + 0.23HCHO + 0.53MGLY + 0.17GLY + 0.17ACET + 0.54CO + 0.46OH + 0.15FACD + 0.4HO_2 + 0.14C2O3$	(R159)	-
(R160)	$ISPD + NO_3 \rightarrow 0.64CO + 0.28HCHO + 0.36ALDX + 1.28PAR + 0.85HO_2 + 0.07CXO3 + 0.07XO2H + 0.07RO2 + 0.85NTR + 0.15HNO_3$	(R160)	$ISPD + NO_3 \rightarrow 0.72HNO_3 + 0.14NTR2 + 0.14NO_2 + 0.14XO2 + 0.14XO2H + 0.11GLYD + 0.11MGLY + 0.72PAR + 0.72CXO3 + 0.28RO2$	(R160)	-
(R161)	$ISPD + h\nu \rightarrow 0.33CO + 0.07ALD2 + 0.9HCHO + 0.83PAR + 0.33HO_2 + 0.7XO2H + 0.7RO2 + 0.97C2O3$	(R161)	$ISPD + h\nu \rightarrow 0.76HO_2 + 0.34XO2H + 0.16XO2 + 0.34MEO2 + 0.21C2O3 + 0.26HCHO + 0.24OLE + 0.24PAR + 0.17ACET + 0.13GLYD + 0.84RO2$	(R161)	-
(R162)	$ISPX + OH \rightarrow 0.9EPOX + 0.93OH + 0.07ISO2 + 0.07RO2 + 0.03IOLE + 0.03ALDX$	(R162)	-	(R162)	-
(R163)		(R163)	$HPLD \rightarrow OH + ISPD + HO_2$	(R163)	$HPLD \rightarrow OH + ISPD$
(R164)		(R164)	$HPLD + NO_3 \rightarrow HNO_3 + ISPD$	(R164)	-
(R165)	$EPOX + OH \rightarrow EPX2 + RO2$	(R165)	-	(R165)	-
(R166)	$EPX2 + HO_2 \rightarrow 0.28GLYD + 0.28GLY + 0.28MGLY + 1.12OH + 0.82HO_2 + 0.38HCHO + 0.07FACD + 0.25CO + 2.17PAR$	(R166)	-	(R166)	-
(R167)	$EPX2 + NO \rightarrow 0.28GLYD + 0.28GLY + 0.28MGLY + 0.12OH + 0.82HO2 + 0.38HCHO + NO_2 + 0.25CO + 2.17PAR$	(R167)	-	(R167)	-
(R168)	$EPX2 + C2O3 \rightarrow 0.22GLYD + 0.22GLY + 0.22MGLY + 0.1OH + 0.66HO2 + 0.3HCHO + 0.2CO + 1.74PAR + 0.8MEO2 + 0.2AACD + 0.8RO2$	(R168)	-	(R168)	-

https://doi.org/10.5194/acp-2020-1295
Preprint. Discussion started: 15 March 2021

Atmospheric Chemistry and Physics Discussions

Table A1. (continued).

Reaction Number	CB6r1	Reaction Number	CB6r2	Reaction Number	CB6r3
(R169)	$EPX2 + RO2 \rightarrow 0.28GLYD + 0.28GLY + 0.28MGLY + 0.12OH + 0.82HO_2 + 0.38HCHO + 0.25CO + 2.17PAR + RO2$	(R169)	-	(R169)	-
(R170)	$INTR + OH \rightarrow 0.63XO2 + 0.37XO2H + RO2 + 0.44NO_2 + 0.18NO_3 + 0.1INTR + 0.59HCHO + 0.33GLYD + 0.18FACD + 2.70PAR + 0.1OLE + 0.08ALDX + 0.27NTR$	(R170)	$INTR + OH \rightarrow 0.63XO2 + 0.37XO2H + RO2 + 0.44NO_2 + 0.18NO_3 + 0.1INTR + 0.59HCHO + 0.33GLYD + 0.18FACD + 2.70PAR + 0.1OLE + 0.08ALDX + 0.27NTR2$	(R170)	-
(R171)	$TERP + O \rightarrow 0.15ALDX + 5.12PAR + TRPRXN$	(R171)	-	(R171)	-
(R172)	$TERP + OH \rightarrow 0.75XO2H + 0.5XO2 + 0.25XO2N + 1.5RO2 + 0.28HCHO + 1.66PAR + 0.47ALDX + TRPRXN$	(R172)	-	(R172)	-
(R173)	$TERP + O_3 \rightarrow 0.57OH + 0.07XO2H + 0.69XO2 + 0.18XO2N + 0.94RO2 + 0.24HCHO + 0.001CO + 7PAR + 0.21ALDX + 0.39CXO3 + TRPRXN$	(R173)	-	(R173)	-
(R174)	$TERP + NO_3 \rightarrow 0.47NO_2 + 0.28XO2H + 0.75XO2 + 0.25XO2N + 1.28RO2 + 0.47ALDX + 0.53NTR + TRPRXN$	(R174)	$TERP + NO_3 \rightarrow 0.47NO_2 + 0.28XO2H + 0.75XO2 + 0.25XO2N + 1.28RO2 + 0.47ALDX + 0.53NTR2 + TRPRXN$	(R174)	-
(R175)	$BENZ + OH \rightarrow 0.53CRES + 0.35BZO2 + 0.35RO2 + 0.12OPEN + 0.12OH + 0.53HO_2 + BENZRO2$	(R175)	-	(R175)	-
(R176)	$BZO2 + NO \rightarrow 0.92NO_2 + 0.08NTR + 0.92GLY + 0.92OPEN + 0.92HO_2$	(R176)	$BZO2 + NO \rightarrow 0.92NO_2 + 0.08NTR2 + 0.92GLY + 0.92OPEN + 0.92HO_2$	(R176)	-
(R177)	$BZO2 + C2O3 \rightarrow GLY + OPEN + HO_2 + MEO2 + RO2$	(R177)	-	(R177)	-
(R178)	$BZO2 + HO_2 \rightarrow$	(R178)	-	(R178)	-
(R179)	$BZO2 + RO2 \rightarrow GLY + OPEN + HO_2 + RO2$	(R179)	-	(R179)	-
(R180)	$TOL + OH \rightarrow 0.18CRES + 0.65TO2 + 0.72RO2 + 0.1OPEN + 0.1OH + 0.07XO2H + 0.18HO_2 + TOLRO2$	(R180)	-	(R180)	-
(R181)	$TO2 + NO \rightarrow 0.86NO_2 + 0.14NTR + 0.42GLY + 0.44MGLY + 0.66OPEN + 0.2XOPN + 0.86HO_2$	(R181)	$TO2 + NO \rightarrow 0.86NO_2 + 0.14NTR2 + 0.42GLY + 0.44MGLY + 0.66OPEN + 0.2XOPN + 0.86HO_2$	(R181)	-
(R182)	$TO2 + C2O3 \rightarrow 0.48GLY + 0.52MGLY + 0.77OPEN + 0.23XOPN + HO_2 + MEO2 + RO2$	(R182)	-	(R182)	-

https://doi.org/10.5194/acp-2020-1295
Preprint. Discussion started: 15 March 2021

Atmospheric Chemistry and Physics Discussions

Table A1. (continued).

Reaction Number	CB6r1	Reaction Number	CB6r2	Reaction Number	CB6r3
(R183)	$TO2 + HO_2 \rightarrow$	(R183)	-	(R183)	-
(R184)	$TO2 + RO2 \rightarrow 0.48GLY + 0.52MGLY + 0.77OPEN + 0.23XOPN + HO_2 + RO2$	(R184)	-	(R184)	-
(R185)	$XYLMN + OH \rightarrow 0.15CRES + 0.54XLO2 + 0.6RO2 + 0.24XOPN + 0.24OH + 0.06XO2H + 0.15HO_2 + XYLRO2$	(R185)	-	(R185)	-
(R186)	$XLO2 + NO \rightarrow 0.86NO_2 + 0.14NTR + 0.22GLY + 0.68MGLY + 0.3OPEN + 0.56XOPN + 0.86HO_2$	(R186)	$XLO2 + NO \rightarrow 0.86NO_2 + 0.14NTR2 + 0.22GLY + 0.68MGLY + 0.3OPEN + 0.56XOPN + 0.86HO_2$	(R186)	-
(R187)	$XLO2 + HO_2 \rightarrow$	(R187)	-	(R187)	-
(R188)	$XLO2 + C2O3 \rightarrow 0.26GLY + 0.77MGLY + 0.35OPEN + 0.65XOPN + HO_2 + MEO2 + RO2$	(R188)	-	(R188)	-
(R189)	$XLO2 + RO2 \rightarrow 0.26GLY + 0.77MGLY + 0.35OPEN + 0.65XOPN + HO_2 + RO_2$	(R189)	-	(R189)	-
(R190)	$CRES + OH \rightarrow 0.06CRO + 0.12XO2H + HO_2 + 0.13OPEN + 0.73CAT1 + 0.06CO + 0.06XO2N + 0.18RO2 + 0.06HCHO$	(R190)	$CRES + OH \rightarrow 0.03GLY + 0.03OPEN + HO_2 + 0.2CRO + 0.73CAT1 + 0.02XO2N + 0.02RO2$	(R190)	-
(R191)	$CRES + NO_3 \rightarrow 0.30CRO + HNO_3 + 0.24XO2 + 0.36XO2H + 0.48ALDX + 0.24HCHO + 0.24MGLY + 0.12OPEN + 0.1XO2N + 0.7RO2 + 0.24CO$	(R191)	$CRES + NO_3 \rightarrow 0.3CRO + HNO_3 + 0.48XO2 + 0.12XO2H + 0.24GLY + 0.24MGLY + 0.48OPO3 + 0.1XO2N + 0.7RO2$	(R191)	-
(R192)	$CRO + NO_2 \rightarrow CRON$	(R192)	-	(R192)	-
(R193)	$CRO + HO_2 \rightarrow CRES$	(R193)	-	(R193)	-
(R194)	$CRON + OH \rightarrow CRNO$	(R194)	$CRON + OH \rightarrow NTR2 + 0.5CRO$	(R194)	-
(R195)	$CRON + NO_3 \rightarrow CRNO + HNO_3$	(R195)	$CRON + NO_3 \rightarrow NTR2 + 0.5CRO + HNO_3$	(R195)	-
(R196)		(R196)	$CRON + h\nu \rightarrow HONO + HO_2 + HCHO + OPEN$	(R196)	-
(R197)	$XOPN + h\nu \rightarrow CAO2 + 0.7HO_2 + 0.7CO + 0.3C2O3 + RO2$	(R197)	$XOPN + h\nu \rightarrow 0.4GLY + XO2H + 0.7HO_2 + 0.7CO + 0.3C2O3$	(R197)	-
(R198)	$XOPN + OH \rightarrow MGLY + CAO2 + XO2H + RO2$	(R198)	$XOPN + OH \rightarrow MGLY + 0.4GLY + 2XO2H + 2RO2$	(R198)	-
(R199)	$XOPN + O_3 \rightarrow 1.2MGLY + 0.5OH + 0.6C2O3 + 0.1ALD2 + 0.5CO + 0.3XO2H + 0.3RO2$	(R199)	-	(R199)	-
(R200)	$XOPN + NO_3 \rightarrow 0.5NO_2 + 0.5NTR + 0.45XO2H + 0.45XO2 + 0.1XO2N + RO2 + 0.25OPEN + 0.25MGLY$	(R200)	$XOPN + NO_3 \rightarrow 0.5NO_2 + 0.5NTR2 + 0.45XO2H + 0.45XO2 + 0.1XO2N + RO2 + 0.25OPEN + 0.25MGLY$	(R200)	-

https://doi.org/10.5194/acp-2020-1295
Preprint. Discussion started: 15 March 2021

Atmospheric Chemistry and Physics Discussions

Table A1. (continued).

Reaction Number	CB6r1	Reaction Number	CB6r2	Reaction Number	CB6r3
(R201)	$OPEN + h\nu \rightarrow OPO3 + HO_2 + CO$	(R201)	-	(R201)	-
(R202)	$OPEN + OH \rightarrow 0.6OPO3 + 0.4RO2 + 0.4CAO2$	(R202)	$OPEN + OH \rightarrow 0.6OPO3 + 0.4XO2H + 0.4RO2 + 0.4GLY$	(R202)	-
(R203)	$OPEN + O_3 \rightarrow 1.4GLY + 0.24MGLY + 0.5OH + 0.12C2O3 + 0.08HCHO + 0.02ALD2 + 1.98CO + 0.56HO_2$	(R203)	-	(R203)	-
(R204)	$OPEN + NO_3 \rightarrow OPO3 + HNO_3$	(R204)	-	(R204)	-
(R205)	$CAT1 + OH \rightarrow CAO2 + RO2$	(R205)	$CAT1 + OH \rightarrow 0.14HCHO + 0.2HO_2 + 0.5CRO$	(R205)	-
(R206)	$CAT1 + NO_3 \rightarrow CRO + HNO_3$	(R206)	-	(R206)	-
(R207)	$OPO3 + NO \rightarrow NO_2 + XO2H + RO2 + ALDX$	(R207)	$OPO3 + NO \rightarrow NO_2 + 0.5GLY + 0.5CO + 0.8HO_2 + 0.2CXO3$	(R207)	-
(R208)	$OPO3 + NO_2 \rightarrow OPAN$	(R208)	-	(R208)	-
(R209)	$OPAN \rightarrow OPO3 + NO_2$	(R209)	-	(R209)	-
(R210)	$OPO3 + HO_2 \rightarrow 0.41PACD + 0.15AACD + 0.15O_3 + 0.44ALDX + 0.44XO2H + 0.44RO2 + 0.44OH$	(R210)	-	(R210)	-
(R211)	$OPO3 + C2O3 \rightarrow MEO2 + XO2 + ALDX + 2RO2$	(R211)	-	(R211)	-
(R212)	$OPO3 + RO2 \rightarrow 0.8XO2H + 0.8ALDX + 1.8RO2 + 0.2AACD$	(R212)	-	(R212)	-
		(R213)	$OPAN + OH \rightarrow 0.5NO_2 + 0.5GLY + CO + 0.5NTR2$	(R213)	-
				(R213)	-
		(R214)	$PANX + OH \rightarrow ALD2 + NO_2$	(R214)	-
				(R215)	$NAPH + OH \rightarrow 0.15CRES + 0.54XLO2 + 0.6RO2 + 0.24XOPN + 0.24OH + 0.06XO2H + 0.15HO_2 + PAHRO2$
				(R216)	$ECH4 + OH \rightarrow MEO2 + RO2$
				(R217)	$XPRP \rightarrow XO2N + RO2$
				(R218)	$XPRP \rightarrow 0.73ACET + 0.27ALDX + 0.27PAR + XO2H + RO2$
				(R219)	$XPAR \rightarrow XO2N + RO2$
				(R220)	$XPAR \rightarrow 0.13ALDX + 0.87ROR + 0.13XO2H + 0.87XO2 + RO2 - 0.13PAR$
		(R215)	$NTR2 \rightarrow HNO_3$	(R221)	-

https://doi.org/10.5194/acp-2020-1295
Preprint. Discussion started: 15 March 2021

Atmospheric Chemistry and Physics Discussions

Table A1. (continued).

Reaction Number	CB6r1	Reaction Number	CB6r2	Reaction Number	CB6r3
(R213)	$CRNO + NO_2 \rightarrow 2NTR$				
(R214)	$CRNO + O_3 \rightarrow CRN2$				
(R215)	$CRN2 + NO \rightarrow CRNO + NO_2$				
(R216)	$CRN2 + HO_2 \rightarrow CRPX$				
(R217)	$CRPX + h\nu \rightarrow CRNO + OH$				
(R218)	$CRPX + OH \rightarrow CRN2$				
(R219)	$CAO2 + NO \rightarrow 0.86NO_2 + 0.14NTR +$ $1.2HO_2 + 0.34HCHO + 0.34CO$				
(R220)	$CAO2 + HO_2 \rightarrow$				
(R221)	$CAO2 + C2O3 \rightarrow HO_2 + 0.4GLY + MEO2 + RO2$				
(R222)	$CAO2 + RO2 \rightarrow HO_2 + 0.4GLY + RO2$				
(R223)	$\rightarrow NO$	(R216)	-	(R222)	-
(R224)	$\rightarrow NO_2$	(R217)	-	(R223)	-
(R225)	$\rightarrow CO$	(R218)	-	(R224)	-
(R226)	$\rightarrow HCHO$	(R219)	-	(R225)	-
(R227)	$\rightarrow ALD_2$	(R220)	-	(R226)	-
(R228)	$\rightarrow IOLE$	(R221)	-	(R227)	-
(R229)	$\rightarrow ALDX$	(R222)	-	(R228)	-
(R230)	$\rightarrow ETH$	(R223)	-	(R229)	-
(R231)	$\rightarrow TOL$	(R224)	-	(R230)	-
(R232)	$\rightarrow XYLMN$	(R225)	-	(R231)	-
(R233)	$\rightarrow ISOP$	(R226)	-	(R232)	-
(R234)	$\rightarrow PAR$	(R227)	-	(R233)	-
(R235)	$\rightarrow OLE$	(R228)	-	(R234)	-